CHAPTER X

Application of Ionic Liquid Materials in Microfluidic Devices

Tugçe Akyazi, Janire Saez, Alexandru Tudor, Colm Delaney, Wayne Francis, Dermot Diamond, Lourdes Basabe-Desmonts, Larisa Florea*, Fernando Benito-Lopez*

X.1 Introduction

Ionic liquids are drawing an increasing interest both in academia and in industry as confirmed by the growing number of publications and patents in the area. [1, 2] Ionic liquids (ILs) are salts, completely constituted of ions with melting temperatures below 100 °C, which is a result of their low-charge density and low symmetry ions. [1, 3-5] ILs are categorised as ''green'' solvents since they are, potentially, green alternatives to volatile organic compounds due to mainly their two outstanding properties: negligible volatility and conventional non flammability. [4-7] Their unique properties are not limited to non-volatility and non-flammability; they have an excellent solvation ability for organic, inorganic and organometallic compounds with improved selectivity, high thermal stability (decomposition temperatures around 300–500 °C), high chemical stabilities (extremely redox robust), and lastly, high ionic conductivity all of which highly extends the variety of their applications. [1-3, 8-15] Nevertheless, other properties, such as biodegradability and toxicity are not yet successfully overtaken, and they should be considered in ILs applications. [7]

One of the main advantages concerning the applicability of ILs is the ability tailor their physical and chemical properties (such as their polarities and affinities, their thermo-physical properties, biodegradation ability or toxicological features, as well as their hydrophobicity and solution behaviours) by a proper manipulation of the cation/anion chemical structure. [16-21] This feature gives them the name of 'designer solvent' and favours their use, particularly in the extraction, separation and analysis of value-added compounds from biomass. [1-3, 21, 22]

Moreover, these tuneable properties are enabling rapid advances in devices and processes for the production, storage and efficient use of energy. [1, 23]

In many applications, the immobilisation of ILs in a solid or semisolid substrate, while keeping their specific properties, is a main requirement in order to generate useful devices. This is possible by the introduction of a new class of hybrid materials, ionogels. Ionogels preserve the important properties of the ILs (liquid-like dynamics and ion mobility) in a solid or a gel like structure, enabling easy shaping, manipulation and integration, increasing remarkably the potential application of ILs in fundamental areas such as energy, environment and analysis. [24, 25]

In recent years, researchers decided to make use of the exceptional features of ILs and ionogels in the microfluidics area and many papers which include the incorporation of ILs materials in microfluidic systems have been published. "Lab-on-a-Chiprefractive indices o" (LOC) / "micro-Total Analysis Systems"(µTAS) or microfluidic (continuous flow, microarray and droplet-based) analysis systems empower the manipulation of fluids at small scales (from a few micrometers up to a millimetre) and small volumes (nL to µL). Microfluidic devices run a series of fluidic unit operations on a platform which is designed with a well-defined fabrication technology and provide a consistent approach for miniaturisation, integration, automation and parallelisation of bio-chemical processes. [26, 27] They have the greatest capability of integration of multiple functional elements into a small structure to produce absolute sample-in/answer-out systems. [26] The incorporation of functionalities such liquid handling, temperature control and detection components for sensing allows fast analysis and improves selectivity compared to conventional devices. [26, 27] Nevertheless, the development of fully integrated microfluidic devices is still facing some compelling obstacles, including fluidic control, miniaturisation and high costs. [26, 28]

Considering the critical requirement of fluid control and fluid transport processes and high detection performance within these platforms, microfluidic devices have adopted a wide range of passively or actively controlled, high performance components, such as microfluidic separators, actuators (valves and pumps), reactors, sample/biomolecule storage, sensing elements which are although sophisticated and achieve their tasks efficiently, are as well costly, highly increasing the price and so decreasing the final market possibilities of microfluidic devices.

Ionic liquids have excellent properties that could be used to improve microfluidic devices, since they are low-cost, easily obtainable materials. Their features make them very good and multifunctional candidates for improving the capabilities of microfluidic devices by building miniaturised / passive microfluidic elements for fluid control, sensing, sample storage, microfluidic separation, microreactors (nanoparticle synthesis), power generators, temperature controllers, electrowetting of surface, etc whereas decreasing the manufacturing costs compared with conventional devices and widens the market possibilities. In this chapter we will look over the fundamental applications of ionic liquids within microfluidic devices. We will summarise ILs integration, focusing on their applicability in microfluidic devices, in order to generate novel

Table1. Ionic liquid names and abbreviations

Ionic liquid name	Abbreviation
triisobutyl(methyl) phosphonium tosylate	$[P_{1,4,4,4}][Tos]$
tetrabutylphosphonium dicyanamide	$[P_{4,4,4,4}][DCA]$
trihexyltetradecyl phosphonium dicyanamide	$[P_{6,6,6,14}][DCA]$
trihexyltetradecyl phosphonium bis(trifluoromethanesulfonyl) imide	$[P_{6,6,6,14}][Ntf_2]$
trihexyltetradecyl phosphonium dodecylbenzenesulfonate	$[P_{6,6,6,14}][DBSA]$
trihexyltetradecyl phosphonium chloride	$[P_{6,6,6,14}][Cl]$
1-Methyl-3-octylimidazolium tetrafluoroborate	$[OMIM][BF_4]$
1-ethyl-3-methyliidazolium methyl sulphate	$[EMIM][MeSO_4]$
1-ethyl-3-methyl imidazolium ethyl sulfate	$[EMIM][EtSO_4]$
1-butyl-3-methylimidazolium hydrogen sulphate	$[BMIM][HSO_4]$

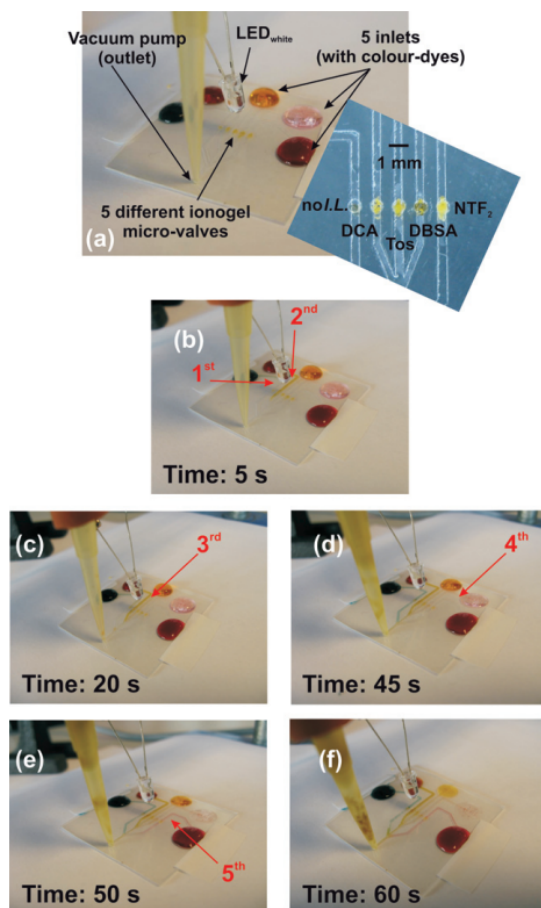| 1-ethyl-3-methyl imidazolium tetrafluoroborate	[EMIM][BF$_4$]
1-ethyl-3-methylimidazolium dicyanamide	[EMIM][DCA]
1-Butyl-3-methylimidazolium tetrafluoroborate	[BMIM][BF$_4$]
1-Butyl-3-methylimidazolium hexafluorophosphate	[BMIM][PF$_6$]
1-Butyl-3-methylimidazolium dodecanesulfonate	[BMIM][DoS]
1-Butyl-3-methylimidazolium bis(trifluoromethanesulfonyl)imide	[BMIM][NTf$_2$]
1-Hexyl-3-methylimidazolium bis(trifluoromethanesulfonyl)imide	[HMIM][NTf$_2$]
1-Buty1-butyl-4-methylpyridinum tetrafluoroborate	[BMPy][BF$_4$]

X.2 Ionic Liquids for Actuators

X.2.1 Microvalves

In 2007 Sugiura *et. al* [29] proposed photo-responsive microfluidic hydrogel valves by copolymerising *N*-isopropylacrylamide (NiPAAm) with a photochromic acrylic benzospiropyran ester (BSP) moiety. Prior to photo-polymerisation, the cocktail mixture of the monomer and the photochromic unit was dissolved in 1-butanol, together with a UV initiator and crosslinker. The photoresponse mechanism of these hydrogels comes as a result of the benzospiropyran moiety present in the copolymer matrix. When the copolymer had been kept in the dark and exposed to an aqueous solution of HCl, the benzospiropyran moiety protonates, changing its conformation to the protonated merocyanine form. When in this conformation, the presence of charges on its backbone contributes to it being more hydrophilic than the closed benzospiropyran conformation. Thus, it absorbs more water and, by irradiating it with white light, it can be reversed to the more hydrophobic benzospiropyran form, together with the release of water. The authors have shown that valves obtained from this material can perform, if preconditioned overnight in acidic conditions, to open and stop the flow inside a poly(dimethyl siloxane) (PDMS) microfluidic device.

Building on this work, Benito-Lopez *et. al* [30] synthesised photo-responsive ionogel valves in microfluidic channels by copolymerising NiPAAm and BSP using a mixture of 1-butanol and phosphonium ionic liquids as the solvent. Four different ILs were used, namely triisobutyl(methyl) phosphonium tosylate ($[P_{1,4,4,4}][Tos]$), trihexyltetradecyl phosphonium dicyanamide ($[P_{6,6,6,14}][DCA]$), trihexyltetradecyl phosphonium bis(trifluoromethanesulfonyl) imide ($[P_{6,6,6,14}][Ntf_2]$), and trihexyltetradecyl phosphonium dodecylbenzenesulfonate ($[P_{6,6,6,14}][DBSA]$), respectively. The resulting crosslinked polymers were left to swell in 1 mM HCl solution for 2 h to reach their maximum swelling capabilities. Following this, they were irradiated with a white light LED until they shrank to their minimum size. In all cases, the time needed for this operation was 100 s. The hydrogel which exhibited maximum shrinking was the control hydrogel, followed by the $[P_{6,6,6,14}][DCA]$, $[P_{1,4,4,4}][Tos]$, $[P_{6,6,6,14}][DBSA]$, and $[P_{6,6,6,14}][Ntf_2]$, respectively. Following this, the monomer mixtures were polymerised in microfluidic devices that featured inlet ports connected to five microchannels which converged into a single microchannel with an outlet port. In each of the five microchannels there was a circular reservoir with a diameter of 500 μm and a height of 175 μm where the monomer mixtures were photopolymerised. The microchannels were 500 μm in width and 50 μm in height. After photopolymerisation, the microfluidic device was flushed with 1 mM HCl to swell the hydrogels. After the hydrogels were swollen and were blocking the channels, a vacuum was applied to the outlet to facilitate the flow and water containing different coloured dyes was placed at each of the inlets. The valves were actuated using a white light LED with a power output of 1 mW·cm^{-2}. Actuation times were 2 s for the control hydrogel, 4 s for the $[P_{6,6,6,14}][DCA]$, 18s for the $[P_{1,4,4,4}][Tos]$, 44 s for the $[P_{6,6,6,14}][DBSA]$, and 49 s for the $[P_{6,6,6,14}][Ntf_2]$ ionogel, respectively (**Figure 1**). This example shows that through the incorporation of different ionic liquids of varying hydrophilic/hydrophobic character, inside ionogel matrices, actuation times can be modulated
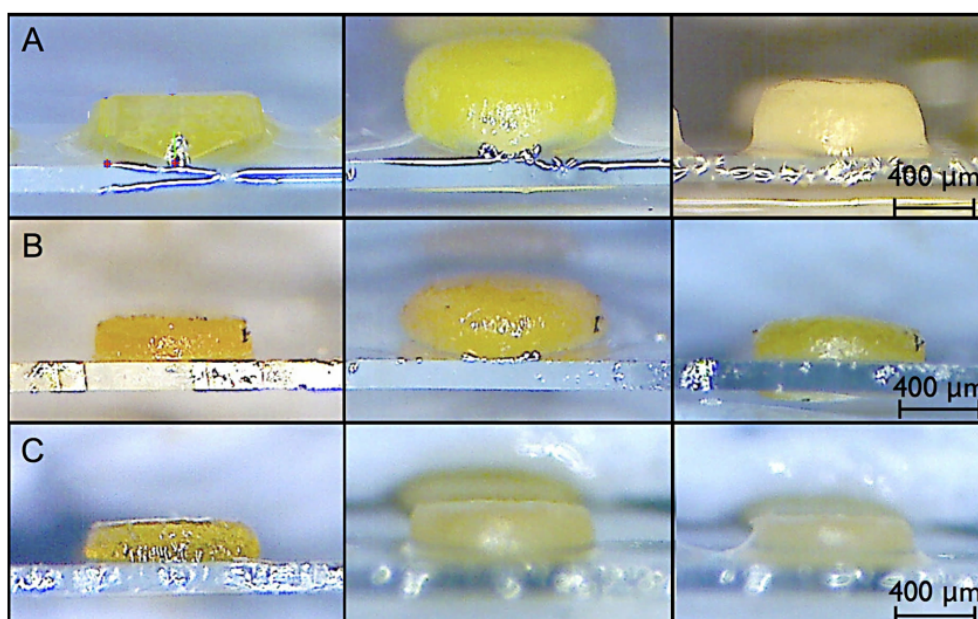
on demand. The time for the hydrogels to revert back to their original size is approximately 30 min, which lead the researchers to conclude that this type of valve would be best suited for single-use devices.

Figure 1. *Image of the microfluidic manifold showing the performance of the ionogel microfluidic valves: (a) all microvalves are closed under the applied vacuum. White light is applied for the time specified in each picture (b) Hydrogel (no IL present) valve is first to actuate followed by ionogels incorporating [DCA]⁻ (c), [Tos]⁻ (d), [DBSA]⁻ (e), [NTf2]⁻ (f). Numbers and arrows indicate when the channel is filled with the dye due to microvalve actuation. Reproduced from Benito-Lopez et al.* [30] *with permission from The Royal Society of Chemistry.*

A more comprehensive study of such photo-responsive ionogel materials was later performed by Czugala *et. al* [31] who studied the photo-responsive behaviour of pNiPAAm-*co*-BSP ionogels made using phosphonium ILs as solvents. Three different phosphonium ILs were chosen for this study: trihexyltetradecyl phosphonium chloride $[P_{6,6,6,14}][Cl]$, $[P_{6,6,6,14}][DCA]$ and $[P_{6,6,6,14}][Ntf_2]$, respectively, and ionogel actuators were photo-polymerised in four different shapes of varying surface area to volume ratios (SA/V): rings, 250 µm discs, 500
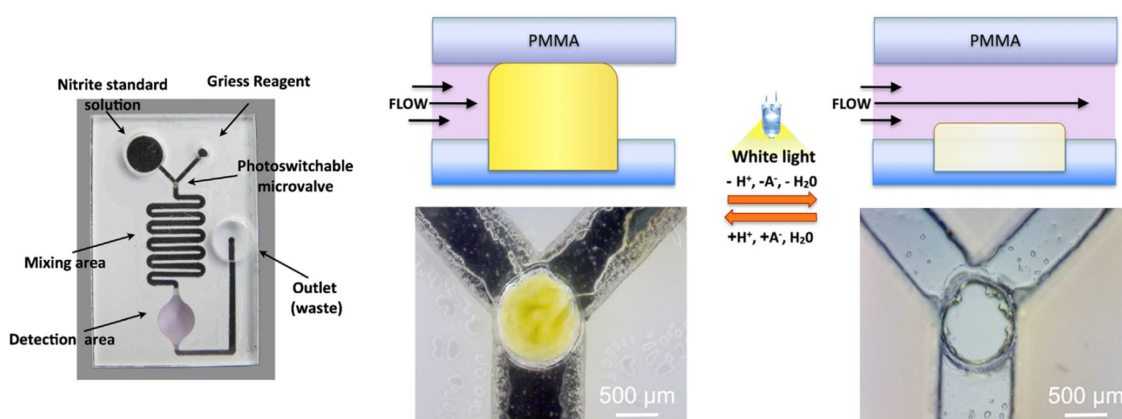
μm discs, and lines, respectively. Their change in size was determined by the change in height, as measured using digital microscopy. By measuring the amount of hydration for each ionogel shape, it was determined that the $[P_{6,6,6,14}][Ntf_2]$ swelled the most, at a value of 109-180 % of the initial gel height (right after photo-polymerisation), followed by $[P_{6,6,6,14}][DCA]$ ionogels (40-58 %), and lastly the $[P_{6,6,6,14}]Cl$ ionogels (20-27 %). Following this, the shrinking behaviour of the ionogels was analysed and it was determined that after 30 min of white light irradiation, the $[P_{6,6,6,14}][Ntf_2]$ ionogels shrunk by 108 %, 15% of their initial height, followed by the $[P_{6,6,6,14}][DCA]$ ionogels shrunk by 42 %, reaching also 15 % of their initial height, while the $[P_{6,6,6,14}]Cl$ ionogels shrunk only by 16 %, reaching 4 % of their initial height (**Figure 2**). The kinetics of the swelling and shrinking behaviours were also determined and in each case the $[P_{6,6,6,14}][Ntf_2]$ ionogels exhibited the highest rates of swelling and shrinking at $(5.3 \pm 0.1) \cdot 10^{-2}$ s and $(29 \pm 4) \cdot 10^{-2}$ s, followed by $[P_{6,6,6,14}][DCA]$ at $(4.5 \pm 0.3) \cdot 10^{-2}$ s and $(8.3 \pm 0.9) \cdot 10^{-2}$ s, and $[P_{6,6,6,14}]Cl$ at $(3.9 \pm 0.2) \cdot 10^{-2}$ s and $(9 \pm 2) \cdot 10^{-2}$ s, respectively. The high swelling and shrinking values attributed to the $[P_{6,6,6,14}][Ntf_2]$ are believed to stem from the fact that this ionic liquid possesses a highly delocalised charge on the S-N-S backbone of the Ntf_2^- anion, which makes it interact less with the charged moieties of the polymer. This leads to more freedom for the polymer backbone to interact with the hydration medium. In the case of the $[P_{6,6,6,14}][Cl]$, this effect is inhibited by the localised charge on the chloride ion, thus associating more strongly to the polymer backbone. The $[P_{6,6,6,14}][DCA]$ ionogels would have an intermediate behaviour between these two states. Based on these results, the $[P_{6,6,6,14}][Ntf_2]$ ionogels were incorporated in a glass-poly(dimethyl siloxane) microfluidic device as light actuated valves. Using a fiber optic to irradiate with white light, the ionogel valve opened after 180 s, allowing liquid to pass through the microfluidic channel. [31]

Figure 2. *Microscope images of ionogel discs made of: (a) [P6,6,6,14][NTf2], (b) [P₆,₆,₆,₁₄][DCA] and (c) [P₆,₆,₆,₁₄][Cl] after photopolymerisation (left); swelling in 1mM HCl solution for 2h (middle) and shrinking upon white light irradiation (right). Reproduced from Czugala et. al [31]. Copyright © 2014 Elsevier B.V. All rights reserved.*

An application of these materials was demonstrated by Czugala *et. al* [32] by using the [P₆,₆,₆,₁₄][DCA] ionogels as photo-responsive valves in a microfluidic analysis platform for the detection of nitrite anions in water. The nitrite assay was done using the Griess reagent and the change in colour was determined using a Paired Emitter Detector Diode (PEDD) arrangement integrated in the microfluidic holder. The emitter diode has a wavelength of 540 nm, while the detector diode has its maximum absorption at 660 nm. Part of the light produced by the emitter diode is absorbed by the Griess-nitrite complex, which has its maximum absorption at 547 nm, while the rest reaches the detector diode and is transformed into a photo current. The amount of photo current generated is proportional to the concentration of nitrite within the sample. By connecting the PEDD setup to a microcontroller fitted with a wireless radio antenna, the data was sent to a PC, where it was stored and analysed. The monomer mixture was photopolymerised using UV light in a circular reservoir with a radius of 500 µm and a height of 225 µm. The reservoir sat at the junction of a Y-shaped microchannel that separated the sample from the Griess reagent
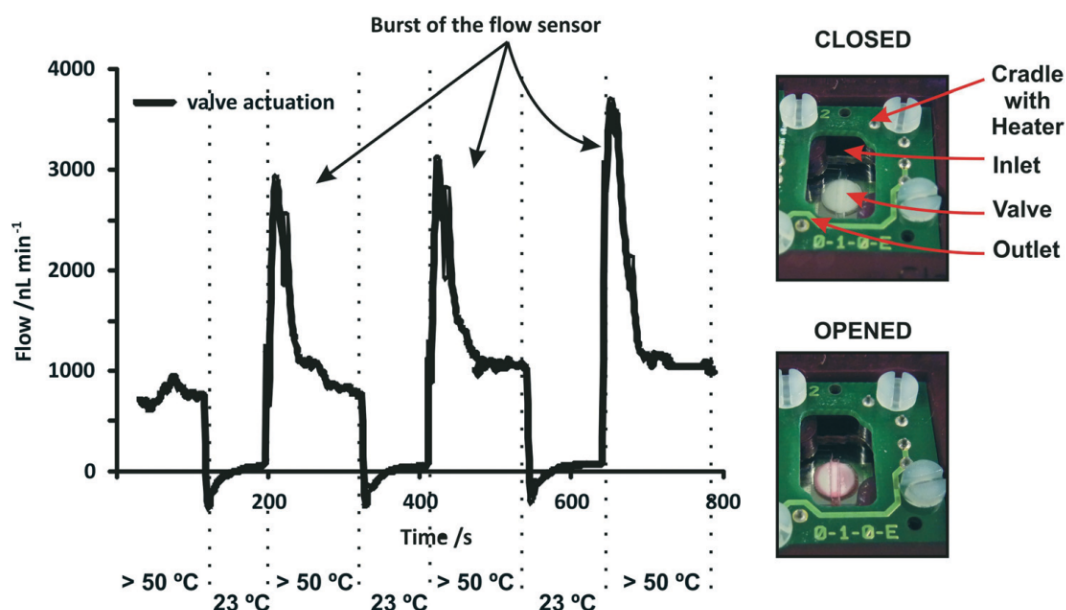
(**Figure 3a**). To operate the valve, the microchannel was filled with 1 mM HCl and left to swell for 2h in the dark. The opening of the valve was performed with irradiation from a white light LED that was also mounted on the microfluidic device holder. By irradiating with a power of 1 mW·cm^{-2}, the ionogel valve opened after 30 ± 5 s (n=3) (**Figure 3b**) and was operated at a pressure of 25 mbar; pressures higher than 31 ± 4 mbar (n=3) deformed the materials and the valves failed. After the ionogel shrunk, the reagent mixture was pumped through the microchannel where it mixed and moved to the detection area for analysis. The calibration curve was made using concentrations of nitrite from 0.2 mg·L^{-1} to 1.2 mg·L^{-1}, in 0.2 mg·L^{-1} steps and performed in triplicate. This yielded a R^2 value of 0.98, a level of detection (LOD) of 34.0 ± 0.1 µg·L^{-1} and a level of quantification (LOQ) of 115 ± 3 µg·L^{-1}, compared to a R^2 value of 0.99, LOD value of 1.50 ± 0.02 µg·L^{-1}, and a LOQ of 14.8 ± 0.2 µg·L^{-1} for a UV-Vis spectrophotometer. The results obtained for the microfluidic platform are lower than the detection limits set by the World Health Organisation. Following this, freshwater samples from the Tolka River in Dublin, Ireland were analysed with both the portable platform and the UV-Vis spectrometer. The close nature of both sets of results proved the suitability of such a microfluidic device and detector for the accurate monitoring of nitrates in real-life samples.

Figure 3. Picture of the microfluidic device fabricated in PMMA: PSA polymer by CO$_2$ laser ablation (left). Schematic (top) and images (bottom) of the photoresponsive microvalve in closed (middle) and opened (right) state. Reproduced from Czugala et. al [32]. Copyright © 2013 Elsevier B.V. All rights reserved.

Thermo-responsive actuation was also proposed for microvalves fabricated using poly(N-isopropylacrylamide) polymer (pNiPAAm) gels. [33] To synthesise these materials, all the components for the monomer mixture were dissolved in 1-ethyl-3-methyl imidazolium ethyl sulfate [EMIM][EtSO$_4$]. The addition of this IL, as demonstrated prior by Gallagher *et. al,* [34] improves the swelling and shrinking capabilities of the pNiPAAm materials, together with lowering the LCST. The microfluidic devices in this study were fabricated using a cutting plotter to cut 100 μm thick layers of cyclic olefin polymer (COP) and thermally bonded, to obtain and microfluidic device with a total area of 1 mm^2 and a total maximum thickness of 1 mm. The resulting microfluidic devices possessed a circular reservoir, which was filled with the monomeric mixture and photopolymerised using UV light. Following this, the resulting microfluidic devices were mounted in a microfluidic holder with an incorporated heating element which could thermally actuate the ionogel valve. The characterisation of the ionogel valves was performed by connecting the inlet of the microfluidic device to a syringe pump with a set flow rate of 1000 nL·min^{-1}, while the outlet was connected to a flow microsensor. Using this experimental setup, the failure pressure of the valves was determined to be 1100 $\pm$ 100 mbar ($n = 5$) and they successfully operated at 200 mbar after being exposed to pressures higher than 1100 mbar. Setting the heating element of the microfluidic holder at a temperature higher than 50 °C, the valves opened 4 $\pm$ 1s ($n = 5$), after the temperature of the ionogel passed its LCST. Recovery was achieved in 32 $\pm$ 2s ($n = 5$), after the temperature dropped below the LCST of the ionogel valves (**Figure 4**). Furthermore, after 10 repetitions, there was no discernable drop in valve performance, showing the potential of these materials as cost-effective reversible valves.
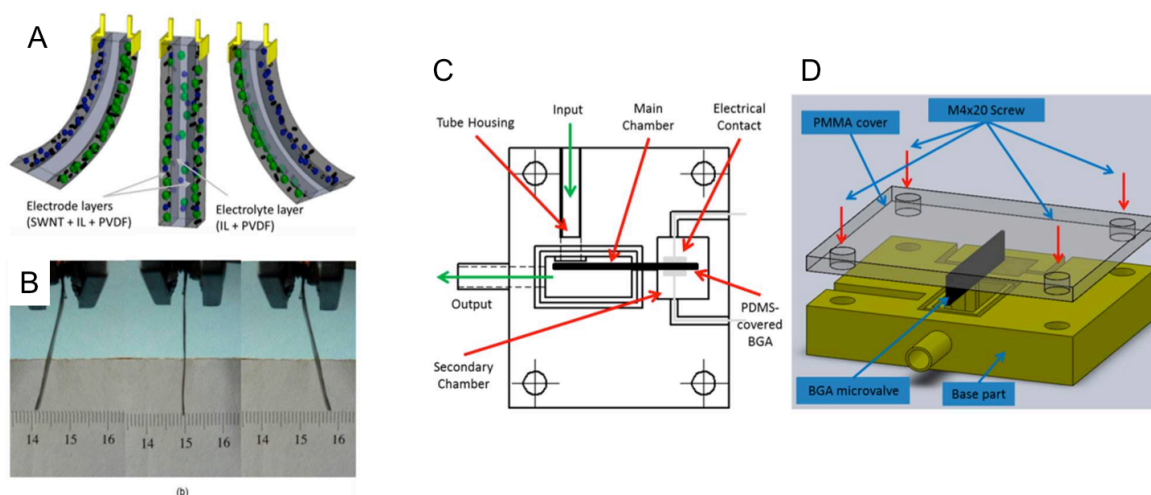
Figure 4. *Flow profile during three full actuation cycles (left) and photo of the microfluidic device containing the thermo-actuated valve and the microfluidic holder with integrated heaters at the bottom. High flow spikes are due to the stabilisation of the microflow sensor after opening of the valve. Reproduced from Benito-Lopez et. al [33] with permission from The Royal Society of Chemistry.*

Electro-actuation of IL based microvalves has also been studied. Ghamsari *et. al* [35] demonstrated the use of bucky gels based on the 1-ethyl-3-methyl imidazolium tetrafluoroborate ionic liquid ([EMIM][BF$_4$]), poly(vinylidene fluoride) (PVDF), and single-walled carbon nanotubes (SWCNT), respectively, as low-voltage microvalve actuators. Bucky gels are gel-like mixtures of carbon nanotubes and ILs which benefit from both the high electrical conductivity associated with carbon nanotubes and the properties of ILs, such as high temperature and electrochemical stability. Bucky gel actuators (BGA) are composite materials which feature a polymer electrolyte core, in this case an ionogel of [EMIM][BF$_4$] and PVDF, inserted between two layers of electrodes made out of bucky gels. Applying voltage to this composite will make it bend in the direction of the applied voltage (**Figure 5a and b**). The electrode components composite was made by mixing all the aforementioned constituents with dimethylacetamide (DMAC) in a ball mill until a black gel mass was obtained. The resulting gel was cast in PDMS moulds and dried until all the DMAC had evaporated. The ionogel layer was fabricated in the same way, without the addition of

SWCNT to the constituent mixture. The resulting layers were then hot-pressed together and covered in a layer of PDMS to increase the adhesion of the resulting BGA to the walls of the microfluidic device, which would ensure better sealing during operation. The actuation properties of the BGA are dependent on the total thickness of the device and on the ratio between the electrolyte layers. Three devices were tested to determine which generates the maximum amount of force by application of a voltage sweep between 4 and 10 V. The devices had thicknesses of 281.9 (BGA1), 322.6 (BGA2), and 393.7 (BGA3), and thickness ratios of 0.73, 1.20, and 0.87, respectively. The results indicated that BGA3 generated a force of 80 mN, which was the highest generated force of the three BGAs. BGA1 and BGA2 generated forces of 38 and 41 mN, respectively. By enclosing the BGAs in a PDMS layer, the forces generated when a voltage is applied are increased between 14 to 23 %. Taking into account that the BGAs will be used in an aqueous medium, a voltage sweep between 2 and 10 V confirmed that there are no bubbles formed due to the hydrolysis. All three BGAs were fitted to microfluidic devices to cover an inlet channel that was fabricated from a tube (**Figure 5c and d**). The tests consisted of using three different operating voltages, namely 5, 8 and 10 V and six different frequencies: 250, 125, 100, 50, 25, and 0 mHz respectively. For all the BGAs, the results indicated that the higher the voltages and the lower the frequency, the better they are suited for use as microfluidic valves. The best results were obtained at 10 V and 0 mHz, at which the flow rate was reduced by 93 %. In all experiments, a leakage flow was present, which led the researchers to determine that the design of the device can be improved to minimise the reoccurrence of this phenomenon.
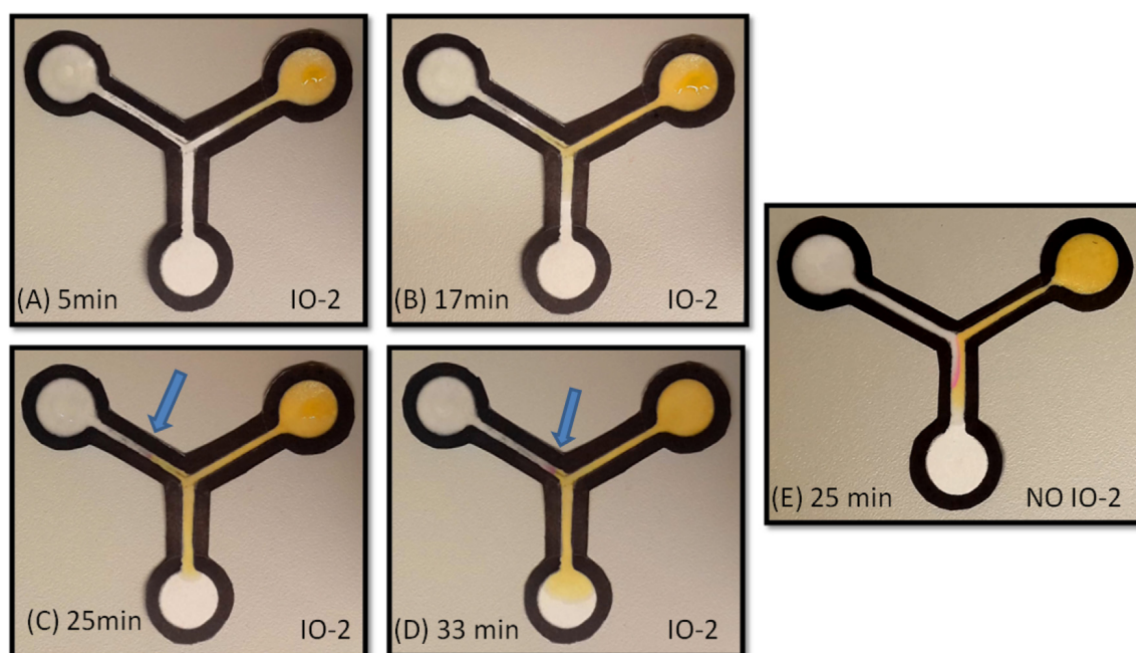
Figure 5. *(a) BGA bending motion as a result of ion transfer between layers; direction of bending can be reversed by changing the polarity of the applied potential; (b) BGA strip bended (10 V, 0.1 Hcolor); (c) Base part and (d) 3D view of the flow regulator assembly. Reprinted with permission from Ghamsari et. al [35]. Copyright 2013 American Chemical Society.*

X.2.2 Delaying pumps

Another application of ILs and ionogels in microfluidic devices include passive pumps where several examples have been proposed in the recent years. In the area of paper-based microfluidic devices, Akyazi *et. al* [36] demonstrated the use of pNiPAAm based ionogels as delaying pumps. Paper is becoming a material of choice in microfluidics due to its ubiquity and low cost, together with attractive physical properties, such as good flexibility, low thickness, low weight, and ability to wick fluids. Its fibrous nature also presents additional challenges with isotropic wicking. The study conducted by Akyazi *et. al* discusses the use of ionogels integrated in paper microfluidic devices to manipulate the wicking properties of these devices. These ionogels were made by dissolving NiPAAm and a crosslinker unit in two different ILs, [EMIM][EtSO$_4$] and [P$_{6,6,6,14}$][DCA], respectively. The paper microfluidic devices (µPADs) were fabricated by ink stamping in triplicate the channels on Whatman Filter paper. After the designs were stamped and dried, the ink provided hydrophobic barriers, which kept the flow of liquid between its limits. The ionogels were

photopolymerised at the ends of the microfluidic devices immediately after application, so that most of the ionogel was formed at the surface of the µPAD. This ensures that the swelling is uniform and the hydrogel will not deteriorate during swelling, while also still being attached to the µPAD. The swelling results indicate that the ionogel synthesised with $[P_{6,6,6,14}][DCA]$ absorbed the most water compared to the $[EMIM][EtSO_4]$ ionogel and the µPAD with no ionogel. Following this, investigations were made to explore the effect of adding an ionogel to one of the channels of a Y-shaped µPAD. The solutions used for this test consisted of a pH = 13 NaOH solution and a pH = 2 H_2SO_4 solution which had methyl red dissolved in it. The pH = 2 solution was added to the right branch of the µPAD, with no ionogel, while the pH = 13 solution was added to the left branch, with the $[P_{6,6,6,14}][DCA]$ ionogel (**Figure 6**). Another Y-shaped µpad without any hydrogels was used as the control. In the case of the control µPAD, the meeting point of the solutions was determined to be in the centre branch of the µPAD, where the colour of the yellow pH = 2 solution changed to purple when it interfaced with the pH = 13 solution. In the case of the µPAD that had the ionogel, the interface between the two solutions formed in the left branch of the µPAD, close to where the $[P_{6,6,6,14}][DCA]$ ionogel resided. After the initial formation of the interface between the two solutions, the interface moved towards the centre branch of the µPAD, due to the constant flow of solution coming from the $[P_{6,6,6,14}][DCA]$ ionogel, after it reached its swelling equilibrium. The use of high and low pH solutions emphasises the fact that the ionogels maintain their function even in harsh conditions. The addition of these materials to paper microfluidic devices increases the usefulness of these devices by decreasing the complexity associated with fluid manipulation, while also being cheap enough to keep costs low.

Figure 6. *A Y-shaped µPAD with photopolymerised [P$_{6,6,6,14}$][DCA] ionogel in the left side inlet after 5 min(A), 17 min (B), 25 min(C), 33 min(D), while injecting NaOH solution (pH=13) in to the left inlet (purple arrow) and phenol red pH indicator and H$_2$SO$_4$ solution (pH = 2) (yellow arrow) into the right inlet. Phenol red gives a pink colour change in a basic environment. (E) a Y-shaped µPAD with no ionogel. Reproduced from Akyazi et al.* [36] *© 2016 Elsevier B.V. All rights reserved.*
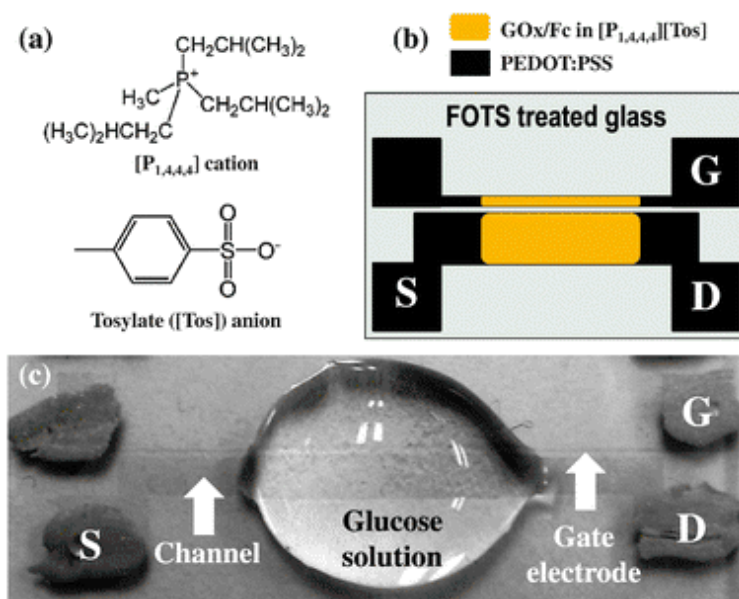
X.3 Ionic Liquids for Sensing

The use of ionic liquids (ILs) for sensing in microfluidic devices continues to gain traction, owed primarily to the ability of these materials to offer a matrix which is capable of responding to chemical and physical stimuli. The wide electrochemical windows, high conductivity, propensity to stabilise enzymes and liquid state at room temperature have carved a particular niche for these exciting new materials in the field of sensing chemical and physical changes. [37] Their ability to immobilise molecules for use in pH analysis, catalysis and electrochemistry have also brought additional application as biomolecular sensors. [38]
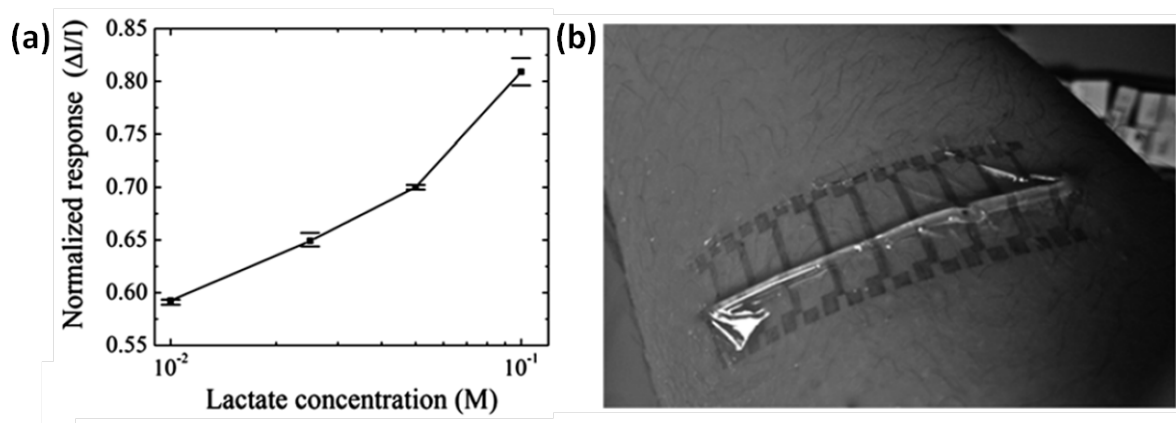
X.3.1 Chemical sensing

The serendipitous growth of point-of-care (POC) technologies, in particular through organic electronics, has buttressed the development of these compounds with a tangible need for

efficient protein solubilisation in specific pH and temperature ranges. One such example, by Yang *et al*. [39] shows recent inroads being made in the field of Organic Electrochemical transistors (OECTs), which have found application in the sensing of ions and antibodies. These simple transistors operate through migration of ions from an electrolyte into a semiconductor, which is often fabricated from a doped polymer, such as poly(3,4-ethylenedioxythiophene) doped with poly(styrene sulfonate) (PEDOT : PSS). By using redox enzymes, such as glucose oxidase in Phosphate Buffer Solution (PBS), it has been possible to achieve micromolar limits of detection. [39] Recent endeavours to use RTILs as a suitable replacement for aqueous electrolytes has brought Yang *et al*. to an IL, namely triisobutyl-(methyl)-phosphonium tosylate [$P_{1,4,4,4}$][Tos], for the fabrication of a new generation of OECTs (**Figure 7**). The hydrophilic nature of the IL, attributed to the tosylate anion, ensures that when patterned over the active area of the OECT, the material subsequently acts as a reservoir for the enzyme and mediator. Upon mixing, the mediator (ferrocene in this case) dissolves, while the enzyme remains dispersed. The presence of this dispersion can have a positive impact on the lifetime of the device by inhibiting a change in the secondary enzyme structure. [40] **Figure 7c** shows that the analyte, in this case a glucose solution forms directly over the area pre-defined by tridecafluoro-1,1,2,2-tetra-hydrooctyl trichlorosilane (FOTS) template. The device, which operates in the 10^{-7}-10^{-2} M range, well within within clinical ranges found in the blood (2–30 mM) and saliva (0.008–0.21 mM) [41] shows great potential for use as a low cost, disposable, POC device.

Figure 7. (a) Chemical structure of [P$_{1,4,4,4}$][Tos]. (b) Schematic of the OECT. (c) Image of the OECT with a drop of glucose solution added. Reproduced from Yang et al. [39] with permission from The Royal Society of Chemistry.
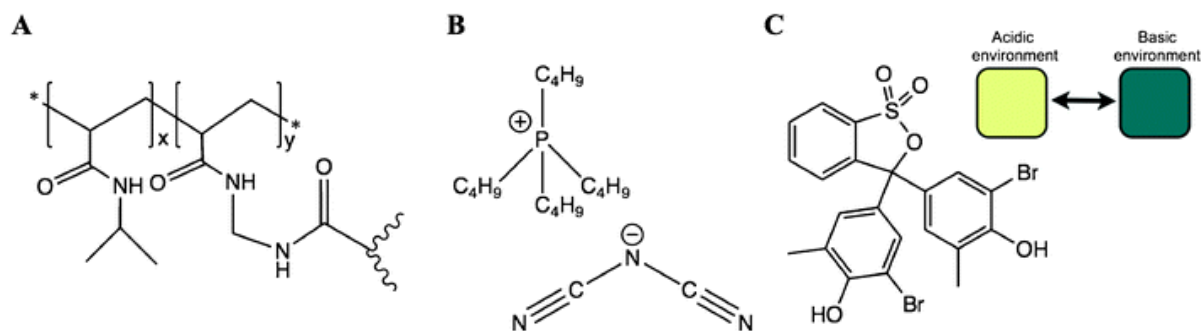
This work has also been developed to sense for other clinically relevant analytes, such as lactate, through incorporation of lactate oxidase (LOx) into an OECT device. [42] In this instance a flexible ionogel based NIPAAm, N,N-methylene-bis(acrylamide) (MBAAm) and [EMIM][EtSO$_4$] incorporating the LOx enzyme was polymerised on the OECT device. As in the case for the glucose sensor, introduction of the specific analyte (in this case lactate), results in an increase in the drain current, which can be directly correlated to lactate concentration, as seen in **Figure 8(a)**. **Figure 8(b)** shows a prototype fabricated from parylene worn on the forearm. [43] Such a flexible prototype, coupled with detection levels suitable for use in the clinical range, prove extremely exciting potential in the fields of sport science and patient care. The conformability of an ionogel incorporated into the OECT device, offers a flexibility not previously possible with more rigid conjugated polymers.

Figure 8. a) Normalised response vs. lactate concentration for the OECT and b) Flexible OECT on the forearm. Adapted from Khodagholy et al. [43] with permission from The Royal Society of Chemistry.
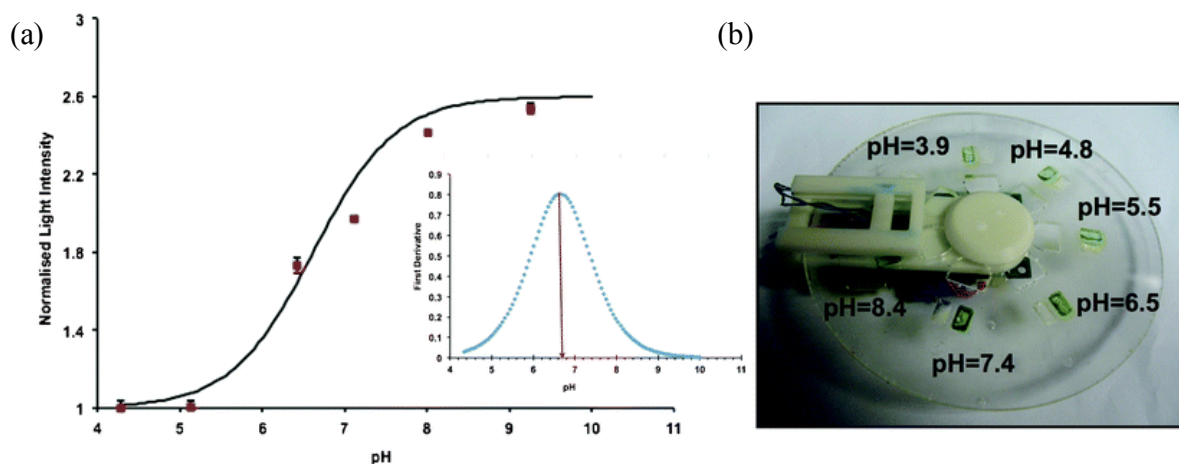
A true understanding of the effect that ILs have on enzymes, has recently been developed by Curto *et al.* [44], in particular for choline-based ILs containing LOx enzyme. They conclude that hydrated ILs can provide the necessary hydrogen bonding for necessary stabilisation of proteins, in addition to controlling the proton buffering within the medium. Interestingly, when stored in choline chloride, over a 140 day period at 5 ºC, 80 % of the initial activity of LOx.

In a similar fashion to the immobilisation of enzymes, ionic liquids can also be used to stabilise other sensing molecules such as dyes. Through ion-pair interactions, a charged dye molecule can be held in the IL or ionogel matrix without leaching. Czugala *et al.* have developed a direct application of such a system, through the use of a centrifugal disc with functionalised ionogel sensing areas. [45] The ionogel, based on poly(N-isopropyl-acrylamide) and N,N'-methylene-bis(acrylamide) and shown **Figure 9(a)** is used to entrap the ionic liquid, tetrabutylphosphonium dicyanamide [P$_{4,4,4,4}$][DCA], and the dye molecule, bromocresol purple (BCP), shown in **Figure 9(b)** and **(c)**, respectively. Photopolymerisation yielded an ionogel, which responds to a variation in pH with the colour change shown in **Figure 9**.

Figure 9. *Chemical structures of A) N-Isopropyl-acrylamide and N,N-methylene-bis(acrylamide) crosslinked polymer; (B) ionic liquid tetrabutylphosphonium dicyanamide [$P_{4,4,4,4}$][DCA] and (C) Bromocresol Purple, showing colour changes in acidic and basic environments. Reproduced from Czugala et al.* [45] *with permission from The Royal Society of Chemistry.*

By development of a light emitting diode (LED) based detector it is possible to generate a colorimetric assay. Optimisation of the concentration of BCP concluded with a 6×10^{-3} M concentration which was used to generate calibration curves across a range of pH values, as shown in **Figure 10**. Moreover, through incorporation of these ionogel materials into a centrifugal disc device, it was possible to include a full colorimetric assay in a CD platform.

Figure 10. *(a) Calibration curve of the sensing area of the microfluidic device using pH buffer solutions; (b) Image of the CD platform with the sensing area. Reproduced from Czugala et al.* [45] *with permission from The Royal Society of Chemistry.*

In a similar fashion, Curto *et al.* [46] have extended the use of IL encapsulated pH responsive dyes to yield a simple barcode device which is capable of measuring sweat pH in real time,

using colorimetric imaging through a mobile phone application (**Figure 11**). In a bid to further extend the lifetime of the microfluidic device, immobilisation of the ionogel on a polymethyl methacrylate (PMMA) substrate was achieved through the use of water plasma treatment, followed by silanisation. The ionogel containing the various dye molecules could then be directly bonded to the functionalised surface, through covalent attachment. By applying an algorithm which mapped to the hue saturation value (HSV) colour space it was then possible to use the mobile phone application to generate calibration curves with R^2 value grater than 0.995.

Figure 11. *(a) Chemical structures of the pH sensitive dyes: Bromophenyl Blue (BPB), Bromocresol Green (BCG), Bromocresol Purple (BCP) and Bromothymol Blue (BTB); (b) Fabricated micro-fluidic device; (c) Smartphone application imaging on-body device. Reproduced from Curto et al.* [46] *with permission from the authors.*

Not only can ionic liquids be used as vehicles for entrapping, immobilising and stabilising sensing materials, such as enzymes, dyes and stimuli responsive materials, they too can be used for their direct interactions with target molecules, most notably in the fields of capillary and microfluidic device electrophoresis. Using ILs as the supporting electrolyte or as additives to the running buffer can dramatically increasing the speed and efficiency of operation, in addition to broadening the range of compounds which can be separated using
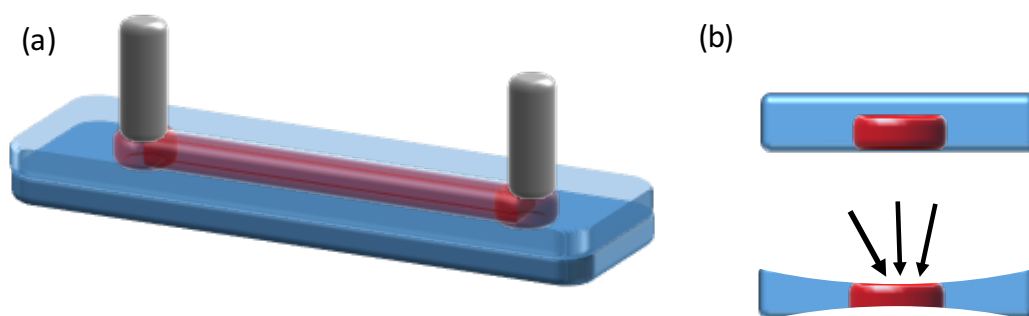
electrophoresis. When used as background electrolytes, in a similar fashion to alkylammonium salts, ILs based on the 1-alkyl-3-methylimidazolium cation were seen to behave as electroosmotic flow modifiers through interaction of the cation either by coating the capillary wall or by migrating into the bulk solution. [47] For the separation of polyphenol compounds in grape extracts the method proved reliable and reproducible. Similarly, for microfluidic device electrophoresis, the use of dynamic coating can prove to be a viable solution to counteract the adsorption of compounds on the hydrophobic polymer materials commonly used for microfluidic fabrication. In the analysis of proteins, for example, surface modification of PDMS channels with ILs, such as 1-butyl-3-methylimidazolium dodecanesulfonate ([BMIM][DoS]) and [EMIM][BF$_4$], can serve to inhibit adsorption of analytes. [48]

X.3.2 Physical sensing

Attributes of ILs, such as good electrical conductivity, high ion density and non-volatility which form the basis for new generations of chemical sensors can also form the basis for much novel work being carried out in the field of physical sensing. Confinement of these conductive liquid materials within a microfluidic channel can generate cheap, pliable and accurate strain-sensors for monitoring motion. These sensors, previously fabricated by casting conductive materials such as silver nanowire, graphene films and carbon nanotubes or through the use of liquid metals within microfluidic channels have generated much recent attention, with the advent of the ubiquitous wearable device. Previous iterations, however, have suffered from complicated fabrication techniques which can result in large hysteresis, resulting in the inability to undergo multiple deformations.

Fabrication of a flexible PDMS channel, filled with a single IL or binary mixture thereof can be used to fabricate thin wearable strain sensors. Matching refractive indices of the binary

mixture can generate a transparent strain sensor, used to measure stretching, bending and other motions. When pressure is applied to the flexible membrane a geometric change within the channel results in an increase of pressure within the channel, thereby leading to a measurable variation in the electrical properties of the ionic liquid (**Figure 12**). These devices can therefore be considered as constant electrofluidic resistors.
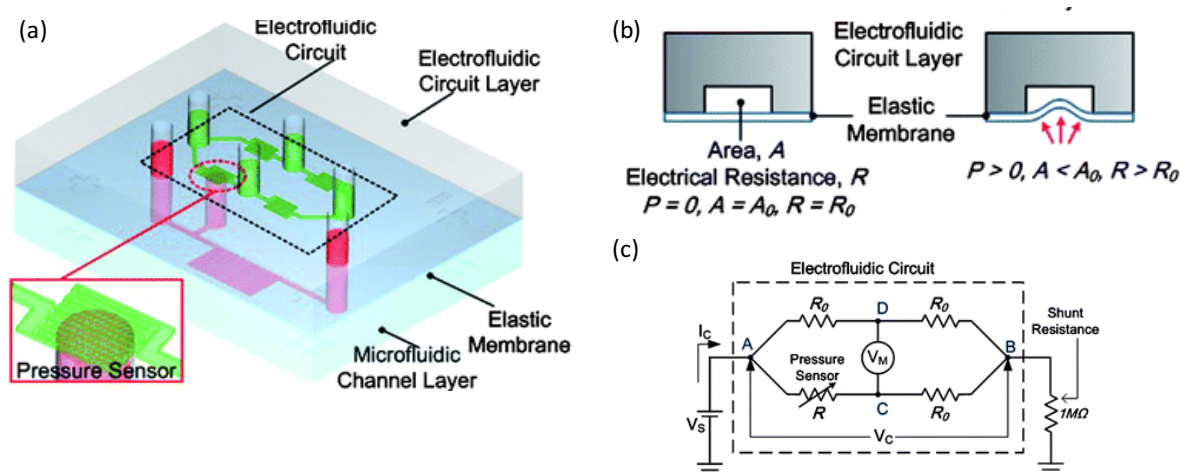

Figure 12. *(a) Representation of simple linear microfluidic strain sensor with platinum electrodes. Red represents the ionic liquid filling the microfluidic channel; (b) Two-dimensional representation of the geometric deformation of the microfluidic channel when pressure is applied.*

Yoon *et al.* [49] described a simple linear channel system of 400 μm width and 70 μm height, filled with a binary mixture (51:49 molar ratio) of 1-butyl-3-methylimidazolium bis-(trifluoromethanesulfonyl)imide ([BMIM][Ntf$_2$]) and 1-butyl-3-methylimidazolium acetate ([BMIM][Ac]). Using platinum electrodes at a constant voltage of 1V (DC) it was possible to monitor current under a range of tensile strain from 10-25 % for multiple cycles. At low strain speeds minimal hysteresis was observed, attributed to the dynamic nature of the IL, thereby eliminating and possible disconnection in the circuit.

This concept has been extended upon in publications such as that by Wu *et al.* [50] to fabricate novel pressure sensors using ILs in similar flexible PDMS channels. Through the use of a bilayer microfluidic device it is possible to use one microfluidic channel as a pressure sensor at a specific location in the second. This change in pressure in the channel filled with 1-ethyl-
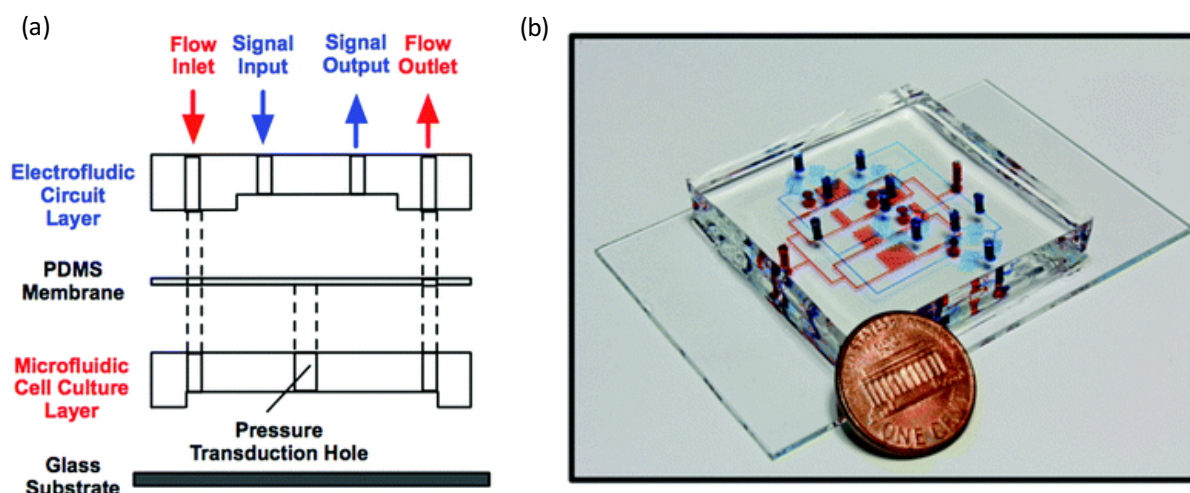
3-methylimidazolium dicyanamide [EMIM][DCA] can be directly related to electrical resistance within the circuit. This change in resistance can be accurately measured through the design of a Wheatstone bridge, as shown in **Figure 13**. Using pressurised gas and liquid in the microfluidic channel it was possible to characterise the sensor, which exhibited impressive thermal stability over extended periods of time. These results displayed much promise for the application of such a device in LOC devices.

Figure 13. (a) Representation of the PDMS microfluidic device showing the microfluidic channel and electrofluidic circuit layers. (b) Conversion of mechanical pressure to electrical resistance. (c) Wheatstone bridge electrofluidic circuit. Reproduced from Wu et al. [50] *with permission from The Royal Society of Chemistry.*

The ability to develop these systems to measure stretch and shear within microfluidic devices has extended their application to devices for microfluidic cell culture, such as Organ-on-a-Chip. These devices can provide a greater understanding of analogous biological processes by monitoring cells in vitro, through real time flow monitoring. Liu *et al.* [51] have developed a microfluidic device for endothelial cell culturing with an embedded pressure sensor (**Figure 14**). Again, by measuring the variation in electrical properties generated from a change in the geometry of the soft-polymer channel filled with [EMIM][DCA], it is possible to determine the pressure within the microfluidic device (**Figure 14**). Such a measurement is critical for

the understanding of the surrounding environment of endothelial cells which are commonly exposed to stress, stretch and hydrostatic pressure.
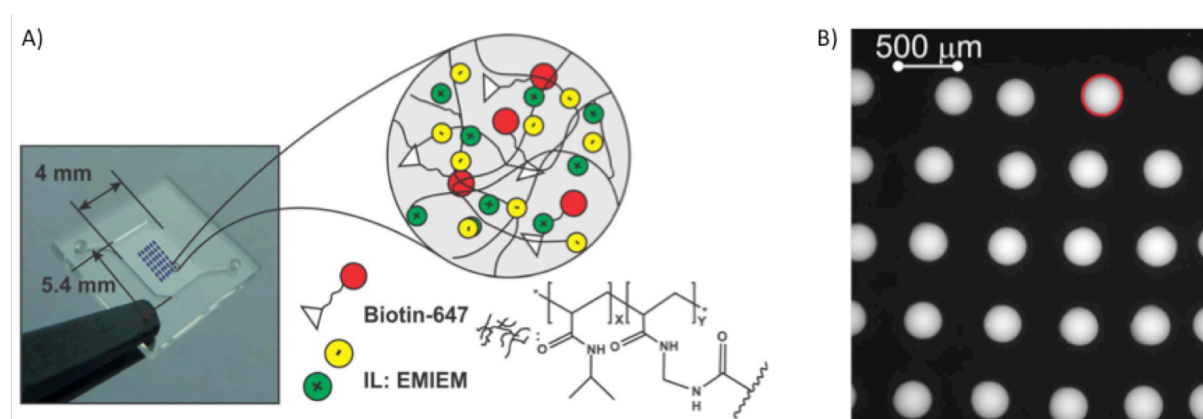

Figure 14. (a) Representation of the microfluidic cell culture showing electrofluidic circuit layer and a microfluidic cell culture layer and glass substrate. (b) Image of the fabricated device showing: the electrofluidic circuit channels (blue) and microfluidic cell culture channels (red). Reproduced from Liu et al. [51] *with permission from The Royal Society of Chemistry.*

X.4 Ionic Liquids for Reagent Storage

Due to their versatility, promising solvation properties and interactions with solute species, ionic liquids have been long proposed as alternative solvents. [52-54] Building up on this and adding their high thermal stability, negligible vapour pressure and enzymatic stability, ionic liquids and ionic liquid gels have been recently proposed as storage media in microfluidic devices. Weidmann *et al.* [55] proposed in 2012, a microfluidic deposition device using ionic liquid matrices which displayed the capability of ionic liquids as matrices for the analysis of biomolecules by MALDI-MS. The microfluidic spotting device addressed several issues of standard protocols employed for MALDI-MS sample preparation such as the co-crystallisation of sample and matrix, clogging and heterogeneity of sample spots. Since the

ionic liquids did not solidify during the measurement, the sample spots remained homogeneous.

Using an ink-jet printing approach, UV-cured ionogel-based microarrays were fabricated and used them for long-term reagent storage of biotin-647 in a LOC device. [56] The ionogel cocktail was based on crosslinked *N*-isopropylacrylamide (NIPAM) and [EMIM][EtSO$_4$] ionic liquid. Biotin-647 was added to this cocktail and the mixture was printed on 6 x 6 array of 300 μm circles (**Figure 15a**) on a variety of untreated substrates such as cyclic olefin copolymer (COC), cyclic olefin polymer (COP), and polypropylene (PP). Following this, the samples were exposed to UV light at 365 nm for 15s to photo-polymerise the printed cocktail and create the final ionogel matrix (**Figure 15b**).

Figure 15. A) Ink-jet printed ionogel microarray in the microfluidic device and representation of the composition of the ionogel spots; B) Fluorescence images of biotin-647 inside an ionogel-based microarray. Reproduced from Tijero et al. [56] *with permission from Springer.*

The viability of this ionogel microarray was demonstrated for biotin-647 storage for over 1 month at room temperature while also proving to effectively keep the activity of biotin-647 in these conditions.

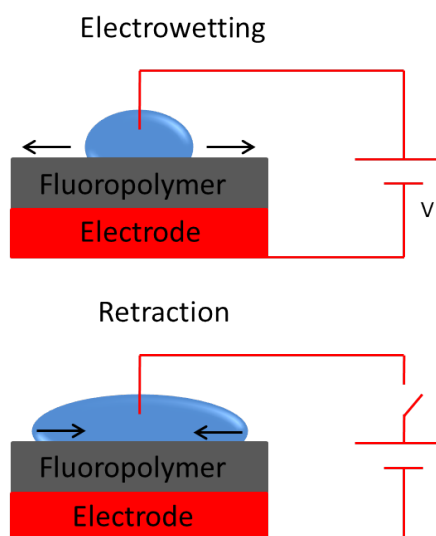**X.5 Ionic liquids in Segmented Flow Microfluidics**

Segmented flow systems offer many exciting and advantageous opportunities in the microfluidic field. Unlike continuous flow microfluidics (which use one single continuous flow), segmented flow devices typically rely on two distinct methods in order to move reagents throughout the microfluidic devices. In the first method, two immiscible flows are forced together at a T-junction, which results in one of the flows becoming the carrier while the second forms droplets. [57] The second method involves the direct manipulation of discrete individual droplets across different types of interfaces (solid-liquid, liquid-air). [58, 59] All segmented flow systems are characterised by a high surface area to volume ratio which results in high heat and mass transfer rates; however, the biggest advantage of these types of flows is the compartmentalisation of reagents into droplets, which allows for control over both the internal and external environment which the reagents are exposed to. Dissociation of reagents from the external environment allows for numerous applications which are not otherwise able to be performed using a continuous flow system, such as having droplets acting as micro-reactors [60], cargo transporters [61], dynamic sensors [62] or drug delivery units [63]. Due to the highly customisable nature of ionic liquids, as well as their high thermal stability and non-combustibility, ionic liquids are ideal candidates for droplet / segmented flow regimes.

X.5.1 Electrowetting on dielectric (EWOD) based microfluidics

Electrowetting on dielectric is the phenomenon by which a discrete droplet can be electrically actuated across a series of electrodes. EWOD is one of the main forms of actuation associated with digital microfluidics and the process involves altering the wettability of a surface via an externally applied electrical field. When the electric field is applied to the device, charges accumulate at the interface between the droplet and solid surface, decreasing the interfacial

tension and thus lowering the contact angle between the droplet and the surface. [64] By addressing sequential electrode pairs in the system, an interfacial tension gradient can be created between neighbouring electrodes, which the droplet will follow to a pre-determined destination. Traditionally, aqueous based droplets have been used in EWOD systems, however due to their high thermal stability, low combustibility and minimal tendencies to corrode the metal parts of the devices, many groups have looked to ILs to replace them. [65-67]

Li *et al.* [68] used high speed video microscopy to investigate the dynamic electrowetting and dewetting capabilities of ILs. In this study they employed five popular imidazolium-based ILs as probe liquids, namely 1-butyl-3-methylimidazolium tetrafluoroborate ([BMIM][BF$_4$]), 1-butyl-3-methylimidazolium hexafluorophosphate ([BMIM][PF$_6$]), [BMIM][NTf$_2$], 1-hexyl-3-methylimidazolium bis(trifluoromethanesulfonyl)imide ([HMIM][NTf$_2$]) and 1-methyl-3-octylimidazolium tetrafluoroborate ([OMIM][BF$_4$]). The focus of this study was to observe the electrowetting at a fixed potential, followed by the dewetting once the potential had been removed. The electrowetting experiments were performed on a fluoropolymer surface (low wettability) under a fixed DC potential of 120 V. Once the electric field was introduced, the base area of the ILs increased exponentially until a maximum area was reached; once the electric field was removed the base area decreased exponentially until they assumed their initial position (**Figure 16**).
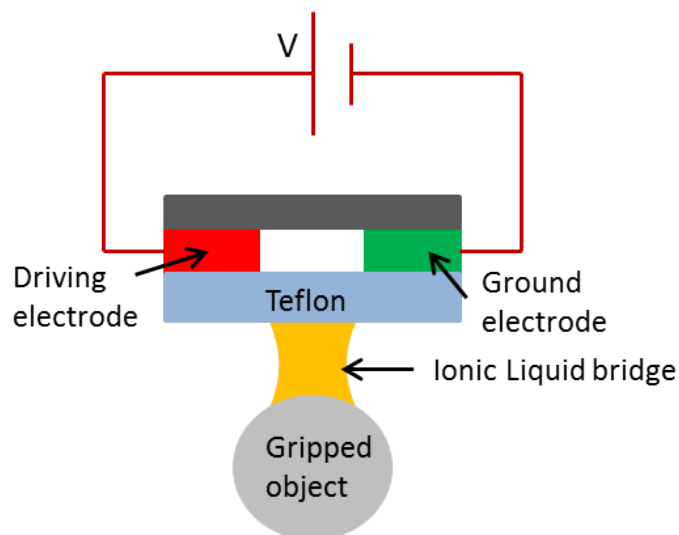
Figure 16. *Illustration of ILs electrowetting and retraction behaviour in the presence (top) and absence (bottom) of a DC potential of 120V. Reproduced from Li et. al* [68]. *Copyright © 2013 Langmuir.*

The IL droplets electrowetting occurred roughly twice as fast as the subsequent retraction, due to the bulky ions within the ILs, which makes it easier to arrange the ions than to destroy their arrangement. The results showed good reversibility which was related to the low contact angle hysteresis of the ionic liquids used. This study showed that ILs can undergo reversible electrowetting behaviour, which added to the fact that ILs show good chemical stability, a large viscosity range and have varying surface tensions, making them ideal for use as electrowetting agents in a variety of applications such as variable focus lenses [69], RC filters [70] and microreactors [60].

Amin *et al.* [71] reported an interesting application for ILs which use their electrowetting capabilities. In this study the group employs ILs as soft micro-grippers in conditions of high temperatures and high vacuum, via electrowetting actuation. The group proposed the use of ILs instead of aqueous droplets as water based systems have a limited functional temperature and vacuum levels while also showing a tendency to erode electrowetting devices. ILs on the other hand, have negligible vapour pressure, high chemical and thermal stability which make them suitable candidates for use in high temperature and vacuum environments. Micro-

grippers are typically used in micro-assembly tasks, where a micro-gripper should be able to pick up, hold and release an item. Classically, capillary forces are used; this is achieved by creating a liquid bridge between the object and the gripper; the capillary forces generated have enough force to lift objects weighing a few milligrams. However, because the capillary force remains constant once the bridge is formed it is difficult to then release the item. The capillary force has to be strong enough to pick up and hold the object for it to be positioned correctly, then the force has to be reduced sufficiently to where it can be released. Amin *et al.* [72] demonstrated that electrowetting could be used to achieve this process, in a procedure similar to the example by Li *et al.* [68] described above. Once the voltage was applied, the surface became hydrophilic, lowering the contact angle of the liquid, which resulted in the formation of a bridge with the object (**Figure 17**). The capillary forces generated allowed for the object to be picked up and held. When the voltage was turned OFF, the surface became hydrophobic and the contact angle of the liquid was lowered, thus releasing the object. The group showed that by using [BMIM][PF$_6$], this process could work in temperatures of up to 110 ºC and vacuums up to 24 inch Hg.

Figure 17. *Cartoon illustration of the ionic liquid micro-gripper.* Reproduced from Al Amin et. al [71]. Copyright © 2011 Journal of Micromechanics and Microengineering. All rights reserved.
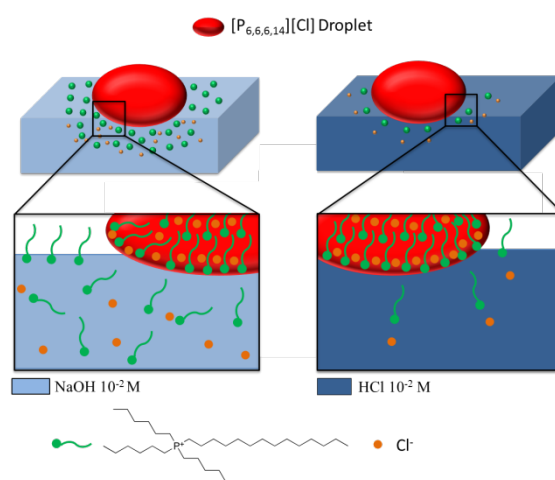
The device functions as follows; firstly the gripper is moved towards the object and a high voltage is applied across the Teflon surface. This makes the surface hydrophilic, allowing the IL to form a bridge, thus creating the maximum force and picking up the object. When the voltage is reduced, the surface becomes hydrophobic, increasing the contact angle of the IL with the surface, reducing the applied capillary forces and releasing the object. The experiments indicated that ILs were ideal for use as micro-grippers in high temperature and high vacuum environments.

X.5.2 Chemotactic Ionic Liquids

Another segmented flow regime involves the actuation of individual droplets across the liquid-air interface through changes in the local surface tension, which is brought upon by the triggered release of a surfactant from the droplet itself. Surfactants are long chained amphiphiles which have hydrophilic "heads" and hydrophobic "tails". When a surfactant is released into an aqueous solution (below the critical micelle concentration) it will interact with polar molecules present at the surface of the solution and will interrupt the attractive forces felt by surface molecules, distributing the local surface tension and creating flows within the bulk solution. Fluid flows from areas of low surface tension to high surface; this is known as the Marangoni effect. By designing systems in which surfactants are asymmetrically released from the droplet into the aqueous phase via external stimulation, droplets have been produced which can solve complex maze designs [73] or can be actuated through white light irradiation [74]. To date, surface tension driven segmented flow systems have mostly focused on aqueous or organic solvent based droplets, which are subject to evaporation and combustion. ILs have a broad range of surface tensions and many have showed surfactant properties [75], while also being highly customisable and overcoming the
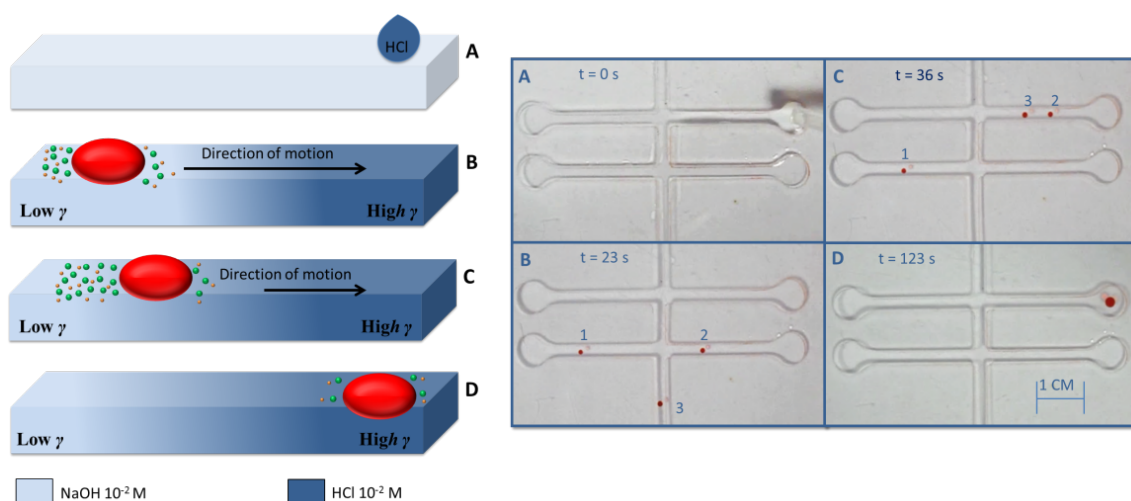
evaporation due to their negligible vapour pressure, making them promising alternatives for aqueous/organic based droplets.

Francis *et al.* [76] were the first to report on the chemotactic movement of ionic liquid droplets composed of [P$_{6,6,6,14}$]Cl. The IL droplets used in this study moved across the liquid-air interface via the triggered release of [P$_{6,6,6,14}$]$^+$, a very effective cationic surfactant and cationic constituent of the IL (**Figure 18**).

Figure 18. *Cartoon illustrating the composition and relative solubility of [P$_{6,6,6,14}$][Cl] in solutions of 10^{-2} M NaOH and 10^{-2} M HCl. Reproduced from 76* with permission from The Royal Society of Chemistry.

When the [P$_{6,6,6,14}$]$^+$ ion diffuses from the droplet into the aqueous solution it interacts with the molecules at the surface, resulting in a drop of the local surface tension. The rate of release of the surfactant is depended on the solubility of the Cl$^-$ counter ion, as any loss of Cl$^-$ ion must also result in an equivalent transfer of [P$_{6,6,6,14}$]$^+$ in order to maintain overall charge neutrality within the droplet. Therefore the rate of release of the counter ion was dependent on the local aqueous Cl$^-$ concentration. Once a droplet of the IL was placed onto a aqueous solution with an imposed Cl$^-$ concentration gradient, there was an asymmetrical release of [P$_{6,6,6,14}$]$^+$ into the aqueous solution, which resulted in the formation of a surface tension gradient around the droplet. This created Marangoni like flows which caused the droplet to move towards areas of highest surface tension (**Figure 19**).

Figure 19. *Illustration showing the chemotactic movement of ionic liquid droplets across the liquid-air interface (left) and sequence of snapshots showing the chemotactic movement of multiple Ionic liquid droplets in an open fluidic channel (right). A – Depicts the creation of Cl⁻ gradient; the channels were initially filled with a solution of 10^{-2} M NaOH and at the desired destination a few drops of a 10^{-2} M solution of HCl were placed. B– Shows the initial placement of the Ionic liquid droplet(s). C – The droplet(s) are propelled towards the highest area of surface tension. D – The droplet arrives at the desired destination. Reproduced from 76 with permission from The Royal Society of Chemistry.*

Francis *et al.* [77] have also demonstrated that ionic liquids can respond to electrical stimuli and show electrotactic movement. Droplet composition and movement remains the same as for the chemotactic ionic liquid droplets described above. In this case, 3D printed electrodes, which were embedded within 3D fluidic channels, were used to generate the required ionic gradients. Francis *et al.* electrotactically actuated droplets of [P$_{6,6,6,14}$][Cl] across the liquid-air interface of 10^{-3} M NaCl electrolyte solutions. This was achieved by imposing an external electric field across the NaCl solution which resulted in the migration of the mobile ions towards their respective counter electrodes. This phenomenon resulted in the formation of a Cl⁻ gradient across the channel, between opposite electrodes. Once the potential was switched ON, an IL droplet placed at the cathode would asymmetrically release surfactant and move towards the anode. By simply reversing the polarity of the electrodes, the gradient and ultimately the droplet movement could be reversed. Moreover, by selectively polarising appropriate electrode pairs the direction of the droplets could be changed and they could be

steered into side channels at junctions (**Figure 20**). The major advantages of electrotactic movement over chemotactic movement of droplets is the ability for concentration gradients to be established and varied dynamically, and maintained for longer periods of time. This resulted in flexible control over the speed and direction of IL droplet movement.

Figure 20. *Series of snapshots which demonstrate the electrotactic movement of IL droplets. Initially the open fluidic channels are filled with a 10^{-3} M solution of NaCl and a potential difference of 9 V is applied across selected electrodes A –introduction of the IL droplet B – D droplet moves away from cathode (3) to anode (1). E – The polarity of electrodes (3) and (1) is reversed and the droplet begins to move to electrode (3). F – As the droplet approaches the junction, the potential difference is applied between electrodes (2) and (4) and removed from electrodes (3) and (1). The droplet then begins to migrate toward anode (2). G – Upon arriving at anode (2) the polarity of electrode (2) and (4) is reversed and the droplet moves towards the new anode (4). H – Upon arriving at anode (4) the potential is again reversed and using a similar method to sequence F the droplet is returned to the starting position. I – L shows the process repeated in the same run. Reproduced from 77 ,*
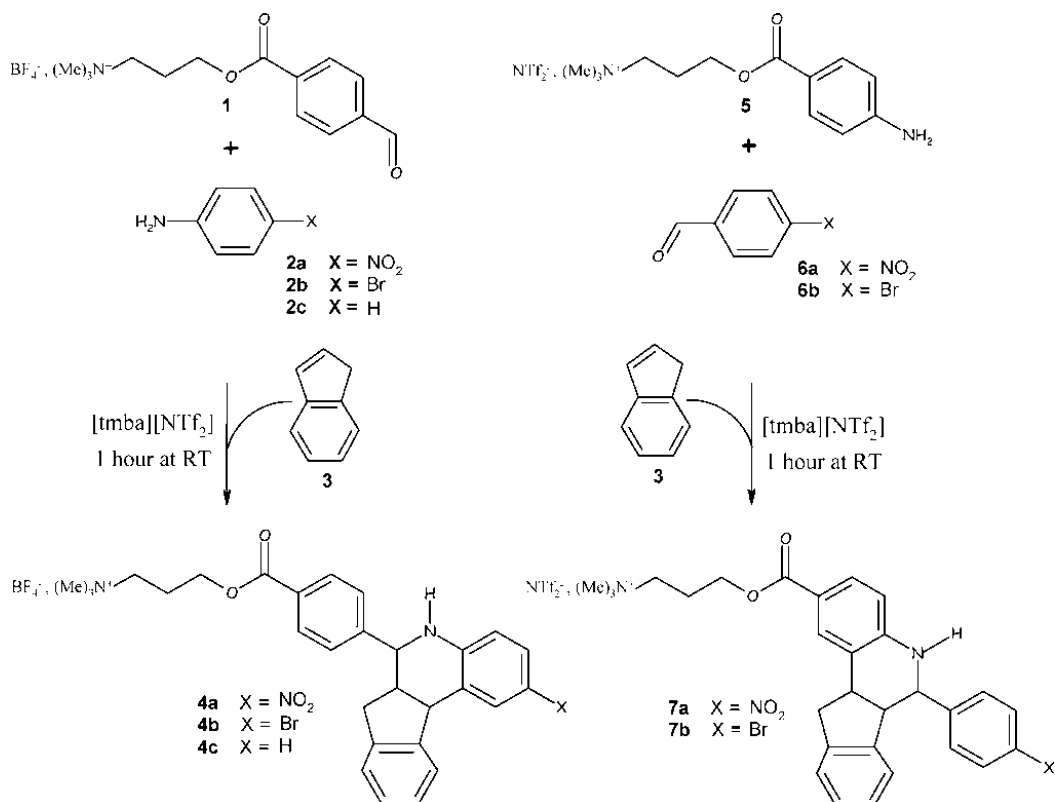
The use of ILs allows for the droplets to remain stable on the surface of the aqueous solutions for much longer than traditional droplets (based on organic solvents) due to their negligible vapour pressure. When coupled with the large (and ever growing) library of ILs available and

the fact that many show surfactant properties, it makes them particularly promising for applications involving autonomous droplet systems such as cargo transporters, sensing units, self-repair agents and drug delivery mechanisms.

X.5.3 Ionic liquids as Microreactors

As mentioned previously, one of the main advantages of segmented flows is the compartmentalisation of the reagents into individual discrete droplets. This has a number of unique properties. Firstly, it separates the reagents from the outside environment, and secondly it allows for the reagents to exist independently of each other within the same device, allowing the user to decide which reagents to mix, when and where. ILs particularly suit this type of application as they have been shown to be excellent solvents [78] and can be tailor made to meet the requirements for many reactions.

Dubois *et al.* [60] reported on the use of IL droplets as microreactors. The ILs were actuated in EWOD devices, in a process similar to the examples described above in which a large number of IL droplets can be efficiently moved and mixed on a Teflon based EWOD device. They also tested the viability of performing complex multi-step reactions using ILs (trimethyl-N-butylammonium bis(trifluoromethylsulfonyl)amide ([tmba][NTf$_2$])) by the synthesis of tetrahydroquinoline, which is a three step synthetic process, **Figure 21**.
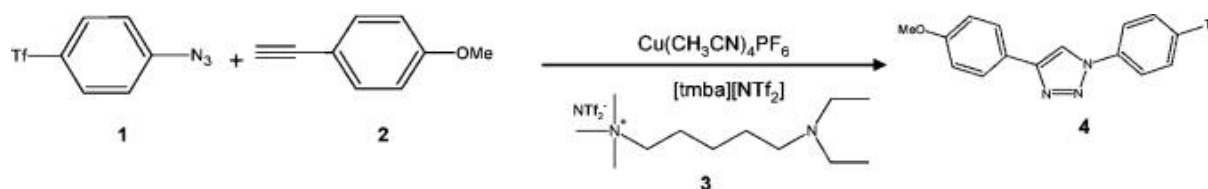
Figure 21. *Reaction scheme for the synthesis of tetrahydroquinoline. Reprinted with permission from 60. Copyright (2006) American Chemical Society.*

As the reaction had two possible reactions routes, both were tested using the IL droplets. To perform the reaction on the EWOD device, a 0.2 μL IL droplet of [tmba][NTf$_2$] which contained 0.2 M of either of the task-specific onium salts (**1** or **2**, **Figure 21**) and 10 equivalents of trifluoroacetic acid (TFA) were placed onto the device. It was then actuated towards a second IL droplet (which contained 2.5 equivalents of either the benzaldehyde derivate (**2**) or the aniline derivate (**6**) by applying 55 V to the corresponding electrodes. Upon merging, the combined droplet was moved to, and merged with a final IL droplet which contained an excess of indene. The droplet was then allowed to incubate for one hour at room temperature. It was then removed and tested via HPLC. The results indicated a near 100 % conversion, comparable with that achieved via conventional methods. Moreover, the group was able to perform the analysis on device by actuating the final reaction droplet to an analytical area where an electrochemical analysis was performed using two gold wires. The signal reflected the concentration of the final product. This paper describes a powerful and

flexible tool which takes advantage of the chemical stability, customisation and non-combustible properties of ILs to perform complex, small scale organic synthesis on a EWOD device.

Marchand *et al.* [78] demonstrated the use of ILs as soft wall-free micro-reactors for organic synthesis via a click reaction. This paper describes the synthesis of fluorescent 1,2,3-triazole by copper-catalysed 1,3 dipolar cycloaddition reaction of azides with terminal acetyls. This reaction (**Figure 22**) is a well-known Click chemistry reaction and results in no by-products and excellent yields.

Figure 22. *Reaction scheme for the synthesis of fluorescent 1,2,3-triazole.* Reprinted with permission from [52]. Copyright (2008) American Chemical Society.

Actuation of the ILs was performed using an EWOD device and various mixing methods. To perform the reaction (without mixing) on the device, a 0.2 µL of the IL ([tmba][NTf$_2$]) which contained 0.2 mol L^{-1} of the azide (**1**) and 0.01 mol L^{-1} of the catalyst (Cu(CH$_3$CN)$_4$PF$_6$) was actuated via electrowetting (55 V) towards, and mixed with a second droplet of the same IL which contained 1 mol L^{-1} of the alkyne (**2**) and 0.03 mol L^{-1} of the support amine (**3**). The reaction was monitored via fluorescence spectroscopy and a 100 % conversion rate was noted after 40 min, which was confirmed via HPLC. This reaction had a long reaction time compared to standard magnetic stirring methods, due to the viscosity of the ILs. In order to overcome this problem, the group tested a number of mixing methods; firstly, the stationary droplet was heated to 40 ºC via a thermoresistor placed under the device. This created Marangoni flows within the droplet, due to the substrate being at a higher temperature than the air, causing the droplet to experience a temperature gradient, which in turn generates a

flow circulation within the droplet. This was proven by monitoring added fluorescent markers to the droplet. The second method involved repeatedly moving the droplet backwards and forwards between a series of electrodes. The final mixing procedure involved positioning the droplet on a module which generated surface acoustic waves (SAW); these waves generate a random and chaotic flow within the droplet which accelerates the mixing of reagents. In all cases the required reaction time was reduced, with the shortest time of 21 min being achieved when mixing via the SAW module was employed. Increasing the temperature decreased the reaction time even further to the point where it was comparable with the orthodox stirring method. This study is important as not only does it show that ILs can be used for small scale organic synthesis (via electrowetting) but it also describes methods to overcome issues with viscosity which can limit the use of ILs in synthesis.

X.6 Ionic Liquids for Separation in Microfluidics

ILs have attracted considerable interest for droplet generation, [79-86] as electrolyte modifiers, [87] biocatalysts [10,11] and in recent years as the continuous phase in two phase microfluidics devices. [90-94] Microfluidic devices allow for the generation of a large number of monodispersed droplets of controlled size. Water immiscible liquids, such as oils and organic solvents, have been used for the formation of micro-droplets in microchannels. [81] However, in order to overcome the limitations of using conventional non-polar solvents (polarity, biomolecule toxicity and device deformation), novel water-immiscible solvents, such as ionic liquids, are being introduced in droplet microfluidics. As an example, Khan *et al.* have presented a general analytical method using imidazolium ionic liquids for 'on-drop' reaction, separation and dynamic reporting. [80] Droplet generation can also be controlled by using magnetic fields. One such example has been reported by Luo *et al.* who demonstrated droplet

formation of a paramagnetic ionic liquid within a magnetic field in a coaxial microfluidic device. [82] Through the application of an external magnetic field they outlined that droplet generation, size and velocity could be controlled. Similarly, Loewe *et al.* have reported the synthesis of monodisperse double emulsions based on organic components and paramagnetic ionic liquids. The external application of magnetic fields allowed for selective and controlled manipulation of emulsion droplets. [83]

Recently, ionic liquids have also been used as liquid electrodes modifiers. [87] Four ionic liquids, 1-butyl-4-methylpyridinum tetrafluoroborate ([BMPy][BF$_4$]), [BMIM][BF$_4$], 1-butyl-3-methylimidazolium hydrogen sulphate ([BMIM][HSO$_4$]), and 1-ethyl-3-methyliidazolium methyl sulphate ([EMIM][MeSO$_4$]) were applied as dynamic modifiers in glass and SU-8 microdevice electrophoresis. This modification allowed for the successful separation of catecholamine derivatives by exploiting the molecular interactions between ionic liquids and catecholamines. He *et al.* developed a dielectrophoresis (DEP) device by using ionic liquids as liquid electrodes, which can be used to continuously separate polystyrene microbeads and PC-3 human prostate cancer cells based on positive DEP. [88] The use of ionic liquids as liquid electrodes has the advantage of low cost and easy fabrication.

The stabilisation of enzymes within ILs has been discussed previously. This forms the basis for the use of ionic liquids as reaction media within enzymatic microreactors. They can facilitate the scale-up of microreactors to industrial scale, providing good adjustability and control over the process. This new field of research in microfluidics has found application in the racemic separation of Ibuprofen from biocatalytic reactors. [89]

Ionic liquids have also been used to replace common volatile organic solvents in aqueous two-phase systems (IL-ATPS). [90] The hydrophobicity and immiscibility of ionic liquids in water allow for their use in the extraction of hydrophobic analytes. As an example, Su *et al.*

developed an IL-ATPS microfluidic chip for the selective extraction of Bisphenol A (BPA) in aqueous samples [91] using *N,N,N*-trioctyl ammonium propionate (TOAP) as the continuous phase. This device showed a 95 % extraction of BPA in 2 s. Moreover, Znidarsic-Plazl *et al.* combined the advantages of the IL-ATPS technique with microfluidics, for the continuous separation of proteins. [92] The hydrophilic IL 1-butyl-3-methylimidazolium tetrafluoroborate ([BMIM][BF$_4$]) and *D*-fructose were employed in an IL-ATPS system with bovine serum albumin (BSA) used as the protein model. Wang *et al.* also worked on protein separation with the use of ionic liquids as extractants. [93] In this case, a water soluble ionic liquid, 1-butyl-3-methylimidazolium dodecanesulfonate ([BMIM][DoS]) was designed and applied to microdevice micellar electrokinetic chromatography (MEKC), possessing both surfactant and IL properties. [BMIM][DoS], which was used as the supporting electrolyte in a microfluidic PDMS device, was found to have a pH of 7.4, making it especially suitable for biological purposes, in addition to preventing adsorption of analytes onto the PDMS surface. Finally, Park *et al.* created an ATPS system for separation in microfluidic devices in which an IL-ATPS device was demonstrated for the effective purification of bacterior-hodopsin (BR) from *Halocaterium salnarium.* [94] The separation of gases has also been achieved using RTILs on Polyethersulfone hollow fibers. [95] The generated membranes were successfully employed for the separation of CO$_2$ and N$_2$ using two different ionic liquids, [BMIM][BF$_4$] and [BMIM][PF$_6$].

Despite the outlined applications, several issues still exist with the use of ILs in microfluidic device separations. These drawbacks, associated with high viscosities, poor fluid and mass transfer of ILs can be circumvented through the use of microencapsulation. Luo *et al.* prepared polysulfone microcapsules filled with [BMIM][PF$_6$] in a microfluidic device. [96] [BMIM][PF$_6$] was successfully encapsulated by polysulfone, to yield small microcapsules with excellent monodispersity and spherical morphology. The authors subsequently

immobilised the same ionic liquids in microcapsules using a mixture of PDMS and *n*-butyl acetate as the continuous phase and polyacrylonitrile and ILs dissolved in *N,N*-dimethylformamide as the dispersed phase. [97] The use of ILs in microfluidic separation allows for the purification of target molecules with rapid purification times and increased yields, in addition to improving the performance of PDMS microfluidic devices by reducing absorption of molecules to the PDMS channel walls.

X.7 Other Applications in Microfluidics

The broad nature of applications using ILs in microfluidic devices makes it difficult to efficiently categorize them independently. The following section presents a compendium of publications, which have not been covered hitherto, in which ILs play an important role for the development and application of microfluidic devices.

X.7.1 Ionic Liquids for Nanoparticle Synthesis in Microfluidics

A particular use for the incorporation of ionic liquids in microfluidic devices is the synthesis of metallic nanoparticles and inorganic nanomaterials. As nanoparticles are an emerging tool in many biomedical applications there is an increasing demand for low cost, rapid, and reproducible nanomanufacturing methods for these materials. [99,100] Microfluidic devices are considered an advantageous option for manufacturing nanoparticles, through continuous flow synthesis. In addition, improved heat and mass transport, fast reagent mixing, continuous throughput, greater reaction control, and minimal solvent waste serve as extremely beneficial attributes. [101,102] These features result in tailor-made nanoparticles of controlled size distribution.[103-107] Recently, ionic liquids, such as those based on dialkylimidazolium cations, have demonstrated promise as both excellent solvents and stabilising ligands for metal nanoparticles while also exhibiting compatibility with PDMS microfluidic devices. [108-110]

Their high ionic charge, high dielectric constant, low interfacial tension and ability to form supramolecular hydrogen-bonded networks in the condensed phase make them ideal solvents for the synthesis and stabilization of metal nanoparticles. [108-112]

Malmstadt *et al.* [113] presented the synthesis of small monodisperse AuNPs using imidazolium-based ILs in a simple PDMS device. It was reported that the nanoparticles owed their high quality to the particle stabilisation effects of the IL solvent working cooperatively with the controlled and fast mixing from the microfluidic device. This technology was used for the fabrication of other high quality nanoparticles through control of reaction parameters, mixing rate and anion of imidazolium IL. The same group fabricated gold and silver nanoparticles in an ionic liquid solvent using a simple droplet-based microfluidic device. [114] They presented a microfluidic platform which brings together a controlled microfluidic mixing with ionic solvents as in their previous work, but this time involving a simplified two-phase droplet flow for the continuous synthesis of high quality, small, monodisperse gold and silver nanoparticles (AuNPs and AgNPs, respectively). This method is reported as an inexpensive, rapid, and reproducible approach which has minimal impact on the environment and opens the possibility of utilising such platforms for high scale nanomanufacturing of nanoparticles.

After the synthesis of metal nanoparticles, the synergistic combination of ionic liquid and droplet microfluidic process was once again adopted for nanomanufacturing of various inorganic materials by Kim and his co workers.[115] Inorganic nanomaterials with unique properties and functions received much recent interest due to their wide variety of applications. [116-118] Despite the many efforts to achieve efficient, fast and continuous synthesis of nanostructured inorganic materials with uniform structure, shape and narrow size distribution, the synthetic process has always been a big challenge. This can be attributed to unmanageable mass and heat transfer and the harsh experimental conditions of high

temperature and pressure. [115, 119, 120] Kim and his team presented a novel droplet-ionic liquid cooperated microfluidic (DIM) synthetic method, which reaps the benefits of both ionic liquids and droplet-assisted microreaction systems, enabling ultrafast, delicate and continuous synthesis of inorganic nanomaterials. [115] This method significantly reduced the reaction time from days to tens of minutes and produced a narrow size distribution and excellent crystalline qualities. As a proof of concept, three nanomaterials ZSM-5, γ-AlOOH, and β-FeOOH were synthesised with the DIM system with excellent quality.

X.7.2 Ionic Liquids for Building Microfluidics-based Power Generator

Kong *et al.* introduced another outstanding application of ionic liquid in microfluidics by building an electrets-based microfluidic power generator (MPG) for harvesting vibrational energy using ionic liquids. [121] It was demonstrated that the MPG with different ILs can generate varying amounts of power, depending on the different variation magnitude of the top contact area. An MPG using IL over water, can operate for longer times in air over a wider range of operating temperatures. This power generator demonstrated the significant potential applications in harvesting low-frequency mechanical vibrations.

X.7.3 Ionic Liquids for Precise Temperature Control in Microfluidics

A novel application, to generate precise and accurate temperature control in microfluidic devices using Joule heating of ionic liquids was presented by Mello *et al.* [122] The relationship between the temperature and conductivity of ionic liquids allows for an internal temperature measurement, with the possibility for application within a thermocouple system. Microfluidic platforms with such fluidic heaters can be easily manufactured, using small amounts of ionic liquid and require no manipulation or replenishment of the heating medium once introduced into the heating microchannel. They also offer extremely long operational lifetimes (estimated order of hundreds of hours). This concept could be used in thermocycling

applications, where integration of multiple heating channels along a co-running reaction microchannel should favor efficient and localised temperature control. Ongoing studies are focusing on the use of these heaters in microfluidic systems for small molecule synthesis within a temperature-controlled environment.

X.8 Conclusions

Lab-on-a-Chip and micro-Total Analysis Systems show great potential for the integration of multiple functional elements, to produce absolute sample-in/answer-out systems. However due to the critical need for fluid control, fluid transport, separation, sensing, the need for high performance microfluidic components can provide significant obstacles for the development of low-cost, miniaturised microfluidic devices. Ionic liquid materials offer a solution for the fabrication of low cost and high performance microfluidic elements which can improve the potential of microfluidic devices. Moreover, the promising results obtained from the use of ILs and microfluidics in separation science and chemical synthesis (nanoparticle generations) provide endless opportunity for this emerging area of research.

X9 Acknowledgements

technological development, and demonstration; through the NAPES project grant agreement no. 604241.

X10 References

1.   M. Petkovic, K. R. Seddon, L. P. N. Rebelo and C. S. Pereira, *Chem. Soc. Rev.*, 2011, 40, 1383-1403.

2.   S. Zhang, J. Wang, X. Lu, Q. Zhou (Eds.), Structures and Interactions of Ionic Liquids 115, in: D. M. P. Mingos (Series Ed.) Structures and Bonding, Springer-Verlag, Berlin-Heidelberg, 2014, pp.1-197.

3.   H. Passos, M. G. Freire and J. A. P. Coutinho, *Green Chem.*, 2014, **16**, 4786-4815.

4.   A. Stark, K.R. Seddon, Ionic liquids, in: A. Seidel (Ed.), Kirk-Othmer Encyclopaedia of Chemical Technology 26, John Wiley & Sons, Inc., Hoboken, New Jersey, 2007, pp. 836-920.

5.   K. R. Seddon, *J. Chem. Technol. Biotechnol.*, 1997, **68**, 351-356.

6.   J. Dupont, P. A. Suarez and A. P. Umpierre, *Catal. Lett.*, 2000, **73**, 11-213.

7.   B. Soares, H. Passos, C. S. R. Freire, J. A. P. Coutinho, A. J. D. Silvestre and M. G. Freire, *Green Chem*., 2016, **18**, 4582-4604.

8.   N. V. Plechkova and K. R. Seddon, *Chem. Soc. Rev.*, 2008, **37**, 23-150.

9.   C. C. Weber, A. F. Masters and T. Maschmeyer, Green Chem., 2013, **15**, 655-2679.

10.   M. J. Earle, J. M. S. S. Esperanca, M. A. Gilea, J. N Canongia- Lopes, L. P. N. Rebelo, J. W. Magee, K. R. Seddon and J. A. Widegren, *Nature*, 2006, **439**, 831-834.

11.   J. S. Wilkes, *Green Chem.*, 2002, **4**, 73-80.

12.   J. M. S. S. Esperanca, J. N. Canongia Lopes, M. Tariq, L. M. N. B. F. Santos, J. W. Magee and L. P. N. Rebelo, *J. Chem. Eng. Data*, 2010, **55**, 3-12.

13.   R. D. Rogers and K. R. Seddon, *Science*, 2003, **302**,792-793.

14.   F. Guo, S. Zhang, J. Wang, B. Teng, T. Zhang and M. Fan, *Curr. Org. Chem.*, 2015, **19**, 455-468.

15.   J. Zhang and A. Bond, Analyst, 2005, 130, 1132-1147.

16.   L. P. N. Rebelo, J. N. C. Lopes, J. M. S. S. Esperanca, H. J. R. Guedes, J. Lachwa, V. Najdanovic-Visak and Z. P. Visak, *Acc. Chem. Res.*, 2007, **40**, 1114-1121.

17.   T. Welton, *Chem. Rev.*, 1999, **99**, 2071-2083.

18.   R. D. Rogers, K. R. Seddon, Ionic liquids 11 IB: Fundamentals, Progress, Challenges, and Opportunities, American Chemical Society Symposium Series, Washington D.C, 2005.

19.   J. Ranke, S. Stolte, R. Stoermann, J. Arning and B. Jastorff, *Chem. Rev.*, 2008, **107**, 2183-2206.

20.   M. Earle and K. Seddon, *Pure Appl. Chem.*, 2000, **72**, 1391-1398.

21.   M. G. Freire, A. F. M. Cláudio, J. M. M. Araújo, J. a. P. Coutinho, I. M. Marrucho, J. N. C. Lopes and L. P. N. Rebelo, *Chem. Soc. Rev.,* 2012, **41**, 4966-4995.

22.   M. G. Freire, A. R. R. Teles, M. A. A. Rocha, B. Schröder, C. M. S. S. Neves, P. J. Carvalho, D. V. Evtuguin, L. M. N. B. F. Santos and J. A. P. Coutinho, J. *Chem. Eng. Data,* 2011, **56,** 4813-4822.

23.   J. F. Wishart, *Energy Environ. Sci.*, 2009, **2**, 956- 961.

24.   J. Le Bideau, L. Viau and A. Vioux, *Chem. Soc. Rev.,* 2011, **40**, 907-925.

25.   P. C. Marr and A. C. Marr, *Green Chem.*, 2016, **18,** 105-128.

26.   C. T. Culbertson, T. G. Mickleburgh, S. A. Stewart-James, K. A. Sellens and M. Pressnall, *Anal. Chem.*, 2014, **86**, 95-118.

27.   E. Livak-Dahl, I. Sinn and M. Burns, *Annu. Rev. Chem. Biomol. Eng.,* 2011, **2**, 325-353.

28.   R. Byrne, F. Benito-Lopez and D. Diamond, *Mater. Today*, 2010, **13**, 16-23.

29.   S. Sugiura, K. Sumaru, K. Ohi, K. Hiroki, T. Takagi and T. Kanamori, *Sens. Actuators, A*, 2007, **140**, 176-184.

30.   F. Benito-Lopez, R. Byrne, A. Răduţă, N. Vrana, G. McGuinness and D. Diamond, *Lab Device*, 2009, **10**, 195-201.

31.   M. Czugala, C. O'Connel, A. McKeon, F. C. Sanchez, X. Munoz-Berbel, A. Llobera, D. Diamond and F. Benito-Lopez, ieee, 2013, DOI: 10.1109/Transducers.2013.6627112, 1695-1698.

32.   M. Czugala, C. Fay, N. E. O'Connor, B. Corcoran, F. Benito-Lopez and D. Diamond, *Talanta*, 2013, **116**, 997-1004.

33.   F. Benito-Lopez, M. Antoñana-Díez, V. F. Curto, D. Diamond and V. Castro-López, *Lab Device*, 2014, **14**, 3530-3538.

34.   S. Gallagher, A. Kavanagh, B. Zíołkowski, L. Florea, D. R. MacFarlane, K. Fraser and D. Diamond, *Phys. Chem. Chem. Phys.*, 2014, **16**, 3610-3616.

35.   A. K. Ghamsari, E. Zegeye, Y. Jin and E. Woldesenbet, *ACS Appl. Mater. Interfaces,* 2013, **5**, 5408-5412.

36.   T. Akyazi, J. Saez, J. Elizalde and F. Benito-Lopez, *Sens. Actuators, B*, 2016, **233**, 402-408.

37.   A. Kavanagh, R. Byrne, D. Diamond and K. J. Fraser, *Membranes*, 2012, **2**, 16.

38.   K. Behera, S. Pandey, A. Kadyan and S. Pandey, *Sensors*, 2015, **15**, 29813.

39.   S. Y. Yang, F. Cicoira, R. Byrne, F. Benito-Lopez, D. Diamond, R. M. Owens and G. G. Malliaras, *Chem. Commun.*, 2010, **46**, 7972-7974.

40.   R. Madeira Lau, M. J. Sorgedrager, G. Carrea, F. van Rantwijk, F. Secundo and R. A. Sheldon, *Green Chem.*, 2004, **6**, 483-487.

41.   M. Yamaguchi, M. Mitsumori and Y. Kano, IEEE Engineering in Medicine and Biology Magazine, 1998, 17, 59-63.

42.   D. Khodagholy, V. F. Curto, K. J. Fraser, M. Gurfinkel, R. Byrne, D. Diamond, G. G. Malliaras, F. Benito-Lopez and R. M. Owens, *J. Mater. Chem.*, 2012, **22**, 4440-4443.

43.   D. Khodagholy, V. F. Curto, K. J. Fraser, M. Gurfinkel, R. Byrne, D. Diamond, G. G. Malliaras, F. Benito-Lopez and R. M. Owens, *J. Mater. Chem*, 2012, **22**, 4440.

44.   V. F. Curto, S. Scheuermann, R. M. Owens, V. Ranganathan, D. R. MacFarlane, F. Benito-Lopez and D. Diamond, *Phys Chem Chem Phys*, 2014, **16**, 1841-1849.

45.   M. Czugala, R. Gorkin Iii, T. Phelan, J. Gaughran, V. F. Curto, J. Ducree, D. Diamond and F. Benito-Lopez, *Lab Device*, 2012, **12**, 5069-5078.

46.   V. F. Curto, C. Fay, S. Coyle, R. Byrne, D. Diamond and F. Benito-Lopez, Seattle Washington, 2011.

47.   E. G. Yanes, S. R. Gratz, M. J. Baldwin, S. E. Robison and A. M. Stalcup, *Anal. Chem.*, 2001, **73**, 3838-3844.

48.   Y. Xu and E. Wang, *J. Chromatogr. A*, 2009, **1216**, 4817-4823.

49.   D. Y. Choi, M. H. Kim, Y. S. Oh, S.-H. Jung, J. H. Jung, H. J. Sung, H. W. Lee and H. M. Lee, *ACS Appl. Mater. Interfaces,* 2016, DOI: 10.1021/acsami.6b12415.

50.   C.-Y. Wu, W.-H. Liao and Y.-C. Tung, *Lab Device*, 2011, **11**, 1740-1746.

51.   M.-C. Liu, H.-C. Shih, J.-G. Wu, T.-W. Weng, C.-Y. Wu, J.-C. Lu and Y.-C. Tung, *Lab Device*, 2013, **13**, 1743-1753.

52.   T. Welton*, Chem. Rev.,* 1999, **99**, 2071-2084.

53.   R. D. Rogers and K. R. Seddon, *Science*, 2003, **302**, 792-793.

54.   W. Kunz and K. Häckl, *Chem. Phys. Lett.*, 2016, **661**, 6-12.

55.   S. Weidmann, S. Kemmerling, S. Mdler, H. Stahlberg and R. Zenobi, *Eur. J. Mass Spectrom.*, 2012, **18**, 279.

56.   M. Tijero, R. Díez-Ahedo, F. Benito-Lopez, L. Basabe-Desmonts, V. Castro-López and A. Valero, *Biomicrofluidics*, 2015, **9**, 044124.

57.   V. van Steijn, M. T. Kreutzer and C. R. Kleijn, *Chem. Eng. Sci.,* 2007, **62**, 7505-7514.

58.   J. Gong, *Lab Device*, 2008, **8**, 898-906.

59.   D. Baigl, *Lab Device*, 2012, **12**, 3637-3653.

60.   P. Dubois, G. Marchand, Y. Fouillet, J. Berthier, T. Douki, F. Hassine, S. Gmouh and M. Vaultier, *Anal. Chem.*, 2006, **78**, 4909-4917.

61.   I. Moon and J. Kim, *Sens. Actuators, B*, 2006, **130**, 537-544.

62.   V. Srinivasan, V. Pamula, M. Pollack and R. Fair, 2003.

63.   Q. Xu, M. Hashimoto, T. T. Dang, T. Hoare, D. S. Kohane, G. M. Whitesides, R. Langer and D. G. Anderson, *Small,* 2009, **5**, 1575-1581.

64.   K. Choi, A. Ng, R. Fobel and A. Wheeler, *Annu. Rev. Anal. Chem.* (Palo Alto Calif.), 2012, **5**, 413-440.

65.   Y. S. Nanayakkara, H. Moon, T. Payagala, A. B. Wijeratne, J. A. Crank, P. S. Sharma and D. W. Armstrong, *Anal. Chem*., 2008, **80**, 7690-7698.

66.   M. Paneru, C. Priest, R. Sedev and J. Ralston, *J. Am. Chem. Soc.,* 2010, **132**, 8301-8308.

67.   S. Millefiorini, A. H. Tkaczyk, R. Sedev, J. Efthimiadis and J. Ralston*, J. Am. Chem. Soc.*, 2006, **128**, 3098-3101.

68.   H. Li, M. Paneru, R. Sedev and J. Ralston, *Langmuir*, 2013, **29**, 2631-2639.

69.   X. Hu, S. Zhang, C. Qu, Q. Zhang, L. Lu, X. Ma, X. Zhang and Y. Deng, *Soft Matter*, 2011, **7**, 5941-5943.

70.   Y. S. Nanayakkara, H. Moon and D. W. Armstrong, *ACS Appl. Mater. Interfaces*, 2010, **2**, 1785-1787.

71.   A. Al Amin, A. Jagtiani, A. Vasudev, J. Hu and J. Zhe, *J Micromech. Microeng.*, 2011, **21**, 125025.

72.   A. Vasudev and J. Zhe, 2008.

73.   I. Lagzi, S. Soh, P. Wesson, K. Browne and B. Grzybowski, *J. Am. Chem. Soc.*, 2010, **132**, 1198-1199.

74.   L. Florea, K. Wagner, P. Wagner, G. G. Wallace, F. Benito-Lopez, D. L. Officer and D. Diamond, *Adv. Mater.*, 2014, **26,** 7339-7345.

75.   J. L. Anderson, V. Pino, E. C. Hagberg, V. V. Sheares and D. W. Armstrong, *Chem. Commun.*, 2003, **87**,2444-2445.

76.   W. Francis, C. Fay, L. Florea and D. Diamond, *Chem. Commun.*, 2015, **51**, 2342 - 2344.

77.   W. Francis, K. Wagner, S. Beirne, D. L. Officer, G. G. Wallace, L. Florea and D. Diamond, Sens. Actuators, B, 2017, **239**, 1069-1075.

20.   M. J. Earle and K. R. Seddon, Pure Appl. Chem., 2000, 72, 1391-1398.

78.   G. Marchand, P. Dubois, C. Delattre, F. Vinet, M. Blanchard-Desce and M. Vaultier, *Anal. Chem.*, 2008, **80**, 6051-6055.

79.   X. Feng, Y. Yi, X. Yu, D-W. Pang, and Z-L. Zhang, LabDevice, 2009, **10**, 313-319.

80.   Z. Barikbin, Md. T. Rahman, P. Parthiban, A. S. Rane, V. Jain, S. Duraiswamy, S. H. S. Lee, and S. A. Khan, Lab Device, 2010, **10**, 2458-2463.

81.   S. Mashaghi, A. Abbaspourrad, D. A. Weitz, and A. M. Van Oijen, Trends Anal. Chem.; TrAC, 2016, **82**, 118-125.

82.   J-P. Huang, X-H. Ge, J-H. Xu, and G-S. Luo, Chem. Eng. Sci., 2016, **152**, 293-300.

83.   V. Misuk, A. Mai, K. Giannopoulos, F. Alobaid, B. Epple, and H. Loewe, Lab Device, 2013, **13**, 4542-4548.84.   L. Bai, Y. Fu, S. Zhao, and Y. Cheng, Chem. Eng. Sci., 2016, **145**, 141-148.

85.   J. W. Hwang, J-H. Choi, B. Choi, G. Lee, S. W. Lee, Y-M. Koo, and W-J. Chang, Korean J. Chem. Eng., 2016, **33**, 57-62.

86.   D. Chatterjee, B. Hetayothin, A. R. Wheeler, D. J. King, and R. L. Garrell, Lab Device, 2005, **6**, 199-206.

87.   I. Alvarez-Martos, F.J. Garcia-Alonso, A. Anillo, P. Arias-Abrodo, M. D. Gutierrez-Alvarez, A. Costa-Garcia, and M.T. Fernandez-Abedul, Sens. Actuators B , 2013, **188,** 837-846.

88.   M. Sun, P. Agarwal, S. Zhao, Y. Zhao, X. Lu, and X. He, Anal. Chem., 2016, **88(16)**, 8264-8271.

89.   Y.S. Huh, Y-Si. Jun, Y.K. Hong, and D.H. Kim, J. Mol. Catal. B: Enzym., 2006, 43, 96-101.

90.   J-P. Fan, J. Cao, X-H. Zhang, and X-K. Ouyang, Sep. Sci. Technol., 2012, **47(12)**, 1740-1747.

91.   L. Qi, Y. Wang, Y. Li, G. Zheng, C. Li, and H. Su, Anal Bioanal Chem, 2015, **407**, 3617-3625.

92.   U. Novak, A. Pohar, I. Plazl, and P. Znidarsic, Sep Purif Technol, 2012, **97**,172-178.

93.   Y. Xu, J. Li, and E. Wang, J. Chromatogr. A, 2008, **1207**, 175-180.

94.   Y.S. Huh, C-M. Jeong, H.N. Chang, S.Y. Lee, W.H. Hong, and T.J. Park, Biomicrofluidics, 2010, **4**, 014103-1-10.

95.   W. Lan, S. Li, J. Xu, and G. Luo, Ind. Eng. Chem. Res., 2013, **52**, 6770-6777.

96.   W.W. Yang, Y.C. Lu, Z.Y. Xiang, and G.S. Luo, React Funct Polym, 2007, **67**, 81-86.

97.   Z.Y. Xiang, Y.C. Lu, Y. Zou, X.C. Gong, and G.S. LuoReact Funct Polym, 2008, **68**, 1260-1265.

98.   Y. Xu, and E. Wang, J. Chromatogr. A, 2009, **1216**, 4817-4823.

99.   C.-H. Chang, B. K. Paul, V. T. Remcho, S. Atre and J. E. Hutchison*, J. Nanopart. Res.*, 2008, **10**, 965.

100.   Y. Song, J. Hormes and C. S. S. R. Kumar, *Small*, 2008, **4**, 698.

101.   A. J. de Mello, *Nature*, 2006, **442**, 394.

102.   H. Song, D. L. Chen and R. F. Ismagilov, *Angew. Chem*., Int. Ed., 2006, **45**, 7336–7356.

103.   Y. Song, H. Modrow, L. L. Henry, C. K. Saw, E. E. Doomes, V. Palshin, J. Hormes and C. S. S. R. Kumar, *Chem. Mater.*, 2006, **18**, 2817.

104.   E. M. Chan, R. A. Mathies and A. P. Alivisatos, *Nano Lett.*, 2003, **3**, 199.

105.   J. Wagner and J. M. Kohler, *Nano Lett.*, 2005, **5**, 685.

106.   S. A. Khan, A. Gunther, M. A. Schmidt and K. F. Jensen, *Langmuir*, 2004, **20**, 8604.

107.   S. Krishnadasan, R. J. C. Brown, A. J. deMello and J. C. deMello, *Lab Device*, 2007, **7**, 1434.

108.   J. Dupont and J. D. Scholten, *Chem. Soc. Rev.*, 2010, **39**, 1780.

109.   M. Neouze, *A. J. Mater. Chem.,* 2010, **20**, 9593–9607.

110.   D. Marquardt, Z. Xie, A. Taubert, R. Thomann andC. Janiak, *Dalton Trans.*, 2011, **40**, 8290–8293.111. J. N. Lee, C. Park and G. M. Whitesides, *Anal. Chem.*, 2003, **75**, 6544-6554.

112.   Ma, Z.; Yu, J.; Dai, S., *Adv. Mater.*, 2010, **22**, 261–285.

113.   L. L. Lazarus, A. S.-J. Yang, S. C. ,R. L. Brutchey and N. Malmstadt, *Lab Device*, 2010, **10**, 3377–3379.

114.   L. L. Lazarus, C. T. Riche, B. C. Marin, M. Gupta, N. Malmstadt and R. L. Brutchey, *ACS Appl. Mater. Interfaces*, 2012, **4**, 3077–3083

115.   P. H. Hoang, H. Park and D. Kim, *J. Am. Chem. Soc.*, 2011, **133**, 14765–14770.

116.   K. J. Van Bommel, C.A Friggeri and S. Shinkai, *S. Angew. Chem., Int. Ed.*, 2003, **42**, 980.

117.   B. L. Cushing, V. L. Kolesnichenko and C. J. O'Connor, *Chem. Rev.*, 2004, **104**, 3893.

118.   Y. Jun, J. Choi and J. Cheon, *Angew. Chem., Int. Ed.*, 2006, **45**, 3414.

119.   A. Abou-Hassan, O. Sandre and V. Cabuil, *Angew. Chem., Int. Ed.*, 2010, **49**, 6268.

120.   S. Duraiswamy and S. A. Khan, *Small*, 2009, **5**, 2828.

121.   W. Kong, L. Cheng, X. He, Z. Xu, X. Ma, Y. He, L. Lu, X. Zhang and Y. Deng*, Microfluid Nanofluid*, 2015, **18**, 1299–1307.

122.   A. J. de Mello, M. Habgood, N. L. Lancaster, T. Welton and R. C. R. Wootton, *Lab Device*, 2004, **4**, 417-419.